Intercomparison of four global precipitation data sets and their correlation with increased Eurasian river discharge to the Arctic Ocean

Tamlin M. Pavelsky[1] and Laurence C. Smith[1]

Received 24 February 2006; revised 16 May 2006; accepted 15 June 2006; published 10 November 2006.

[1] Recent increases in Eurasian river discharge to the Arctic Ocean have attracted considerable scientific attention but remain poorly understood. Previous studies have examined fire frequency, permafrost thaw, and dam construction as potential mechanisms. Here we focus on precipitation as a driver, using 198 dam-free Eurasian river basins ranging from 151 to 897,000 km^2. Using R-ArcticNet monthly discharge data and four observational and reanalysis precipitation products from the University of Delaware (UDel), University of Washington (UW), NCEP/NCAR (NCEP), and ECMWF (ERA-40), we (1) assess which precipitation data sets best capture spatially realistic patterns as inferred from agreement with river discharge (198 basins; 1958–1989); and (2) determine to what extent observed discharge trends follow Udel precipitation changes (66 basins; 1936–1999). Results from the precipitation intercomparison show for the 74 (of 198) basins displaying statistically significant discharge trends (24 positive, 50 negative; −74% to +89%, mean = −1%), interpolated precipitation products significantly outperform reanalysis data sets, perhaps owing to the fine-scale resolutions examined here. Agreement between discharge and precipitation is 42–86% and 42–97% for UDel and UW, respectively, but approaches zero for NCEP and ERA-40. Comparison of precipitation and discharge trends suggests that precipitation increases play a significant role in observed long-term discharge increases. For the 40 (of 66) basins displaying statistically significant trends in discharge (32 positive, 8 negative; −23% to +50%, mean = +11%), 29 display corresponding trends in precipitation with 35–62% agreement between discharge and precipitation trend. Comparison of discharge trends with basin permafrost properties indicates a possible, but not strong role for permafrost thaw in the observed increases.

Citation: Pavelsky, T. M., and L. C. Smith (2006), Intercomparison of four global precipitation data sets and their correlation with increased Eurasian river discharge to the Arctic Ocean, *J. Geophys. Res.*, *111*, D21112, doi:10.1029/2006JD007230.

1. Introduction

[2] The Arctic has received substantial attention in recent years as a region exhibiting rapid warming as well as for its influence on the global climate system [*IPCC*, 2001; *ACIA*, 2005]. Increases in temperature of as much as 5°C per decade in some areas make the Arctic among the most rapidly warming regions globally [*Hinzman et al.*, 2005; *Serreze et al.*, 2000]. These temperature increases are associated with increased moisture transport from low to high latitudes [*Manabe and Stouffer*, 1995], an important factor in influencing Arctic precipitation variability. Terrestrial runoff, in turn, influences both regional and global climate. The freshwater budget of the Arctic Ocean is significantly influenced by river discharge, with 11% of the global river discharge entering an ocean basin containing only 2% of global ocean water [*Steele et al.*, 1996; *Aagard and Carmack*, 1989]. As such, oceanic processes may be significantly affected by hydrologic changes over adjacent landmasses [*H. Ye et al.*, 2003]. Specifically, recent observations of acceleration in the Arctic water cycle suggest that sea ice will retreat and sea surface temperatures will rise as the Arctic Ocean becomes fresher [*H. Ye et al.*, 2003; *Serreze et al.*, 2000], while formation of North Atlantic Deep Water (NADW) may decrease and consequently slow thermohaline circulation in the Atlantic [*Peterson et al.*, 2002; *Manabe and Stouffer*, 1995; *Rahmstorf*, 1995]. Some studies suggest that this process may have begun already [*Curry et al.*, 2003; *Dickson et al.*, 2002; *Bryden et al.*, 2005].

[3] Of particular interest are the recently observed and modeled increases of approximately 1% per decade in Siberian river discharge between 1936 and 1999 [*Peterson et al.*, 2002; *Wu et al.*, 2005]. If the rate of runoff increase is associated with temperature rise, as suggested by general circulation and hydrologic models, then Eurasian river discharge to the Arctic Ocean may increase 40–70% over the next 100 years [*Peterson et al.*, 2002; *Manabe et al.*, 2004; *Lawrence and Slater*, 2005], potentially shutting down NADW formation by early in the next century

[1]Department of Geography, University of California, Los Angeles, Los Angeles, California, USA.

0148-0227/06/2006JD007230

[*Peterson et al.*, 2002]. However, the physical mechanism(s) driving the runoff increases are not well understood. Several hypotheses have been posited, including thawing of permafrost [*Oelke et al.*, 2004; *Zhang et al.*, 1999, 2000], increased forest fire frequency, and the influence of dam construction [*McClelland et al.*, 2004]. It is unlikely, however, that any of these can explain more than a small proportion of the observed annual discharge increases, though they may play a role in changing seasonal discharge patterns [*McClelland et al.*, 2004]. *Lawrence and Slater* [2005], for example, suggest that perhaps 15% of discharge increases to the Arctic Ocean are related to melting ground ice. On the global scale, a decreased rate of plant transpiration as a result of increased atmospheric CO_2 concentrations has also been suggested as a possible mechanism for increasing river discharge [*Gedney et al.*, 2006], though the scale of the study is vastly different from that applied here and thus the implications are uncertain. The most likely explanation, then, is increased net transport of atmospheric moisture into the Eurasian Arctic resulting in higher precipitation [*Peterson et al.*, 2002; *McClelland et al.*, 2004; *Lawrence and Slater*, 2005].

[4] Large uncertainties in precipitation estimates, however, make this hypothesis difficult to test [*Serreze et al.*, 2003; *Berezovskaya et al.*, 2004; *McClelland et al.*, 2004]. The precipitation gauge network in the Eurasian Arctic is sparse, making interpolation between distant stations necessary for many areas [*Serreze et al.*, 2003]. Additionally, widespread differences in gauge efficiency due to variations in wind speed and equipment may lead to measurement errors as high as 50–100% for solid precipitation in some regions [*Groisman et al.*, 1991; *Yang and Ohata*, 2001]. Corrections for these biases are difficult, and little agreement exists within the community on how best to address them [*Yang et al.*, 2005; *Serreze and Etringer*, 2003; *Groisman and Rankova*, 2001; *Adam and Lettenmaier*, 2003]. Additionally, substantial declines in the number of high-latitude precipitation and discharge observations since approximately 1990 make analysis of recent trends somewhat difficult [*Serreze et al.*, 2003; *Adam and Lettenmaier*, 2003; *Shiklomanov et al.*, 2002].

[5] Many studies examining linkages between precipitation and discharge have used gridded runoff data sets with hydrologic models to examine pan-Arctic or pan-Eurasian hydrologic variability, eschewing the use of river basins as a basic unit of analysis entirely [*Rawlins et al.*, 2003; *Serreze et al.*, 2002; *Fekete et al.*, 2004; *Ye et al.*, 2004; *Georgievskii et al.*, 1996]. Those studies that do use basins have focused only on the largest watersheds, especially the Ob', Lena, and Yenisey basins [*Peterson et al.*, 2002; *Berezovskaya et al.*, 2004; *McClelland et al.*, 2004; *Serreze et al.*, 2002]. This focus on very large scales of variability has to some degree limited the possibility of observing finer-scale patterns in discharge-precipitation relationships. Furthermore, use of only a few basins limits statistical analysis owing to small sample size. A handful of studies have examined smaller subbasins of these large catchments [*Yang et al.*, 2004a, 2004b, 2002; *B. Ye et al.*, 2003], but each of these studies has focused on a subsection of northern Eurasia, and they do not attempt to incorporate the statistical approaches used here. As a result, past studies have been somewhat inconclusive in determining whether precipitation is a principle driver of the observed discharge increases [*Berezovskaya et al.*, 2004; *Serreze et al.*, 2002; *Ye et al.*, 2004]. Results from the Canadian Arctic suggest that a recently observed 10% decrease in total annual river discharge between 1964 and 2003 is entirely consistent with a corresponding decline in precipitation [*Dery and Wood*, 2004, 2005].

[6] Here we examine relationships between annual precipitation and discharge in 198 river basins across the Eurasian Arctic, many of which are subbasins of those examined by *Peterson et al.* [2002] and others (Figure 1). Basins range in size from 151 to 897000 km^2 and were chosen to be free from the influence of dams. Discharge observations for these basins are available in the R-ArcticNet v. 3.0 database of monthly river discharge, which contains runoff data for several thousand basins across the Arctic [*Lammers et al.*, 2001]. Also examined were four widely used observational and reanalysis precipitation data sets released by the University of Delaware (UDel) [*Willmott and Matsuura*, 2001], University of Washington (UW) [*Adam and Lettenmaier*, 2003], European Center for Medium Range Weather Forecasting ERA-40 Reanalysis Project (ERA-40) [*Simmons and Gibson*, 2000], and the National Center for Environmental Prediction/National Center for Atmospheric Research (NCEP) [*Kistler et al.*, 2001] (Table 1). An intercomparison of these four precipitation products with the observed discharge time series over the period common to all four (1958 to 1989) forms the first part of this paper. We attempt to assess which of the data sets best represent spatially realistic values of precipitation as inferred from their agreement with spatial patterns in river discharge. In the second part of the paper, we use the long-term UDel precipitation data set to estimate the contributions of precipitation to observed discharge trends for 66 basins with long records of river discharge (1936–1999) in order to determine the role of precipitation in the observed 20th century increases in river outflow.

2. Data and Methods

[7] The data and methods section is divided into five subsections. The first two describe the discharge and precipitation data sets. The delineation of river basin boundaries using topographic and hydrologic data is described next. The fourth subsection presents the methodology used to evaluate the four precipitation data sets examined in this study, while the fifth and final subsection describes the techniques used to evaluate precipitation as a driver of discharge change as well as the influence of permafrost extent on discharge trend.

2.1. Discharge Data

[8] We examined 198 basins for water years (October through September) 1958 to 1989 and a subset of 66 basins for water years 1936 to 1999. Annual values of river discharge for each of the 198 watersheds were aggregated from R-ArcticNet 3.0 monthly discharge data [*Lammers et al.*, 2001]. The criteria used to select test basins from the several thousand available in the full database are (1) no influence from major dam construction, (2) ultimate drainage to the Arctic Ocean, and (3) at least 90% completion of the data record for each month. Eighteen basins in very flat areas were excluded because of difficulties in correctly

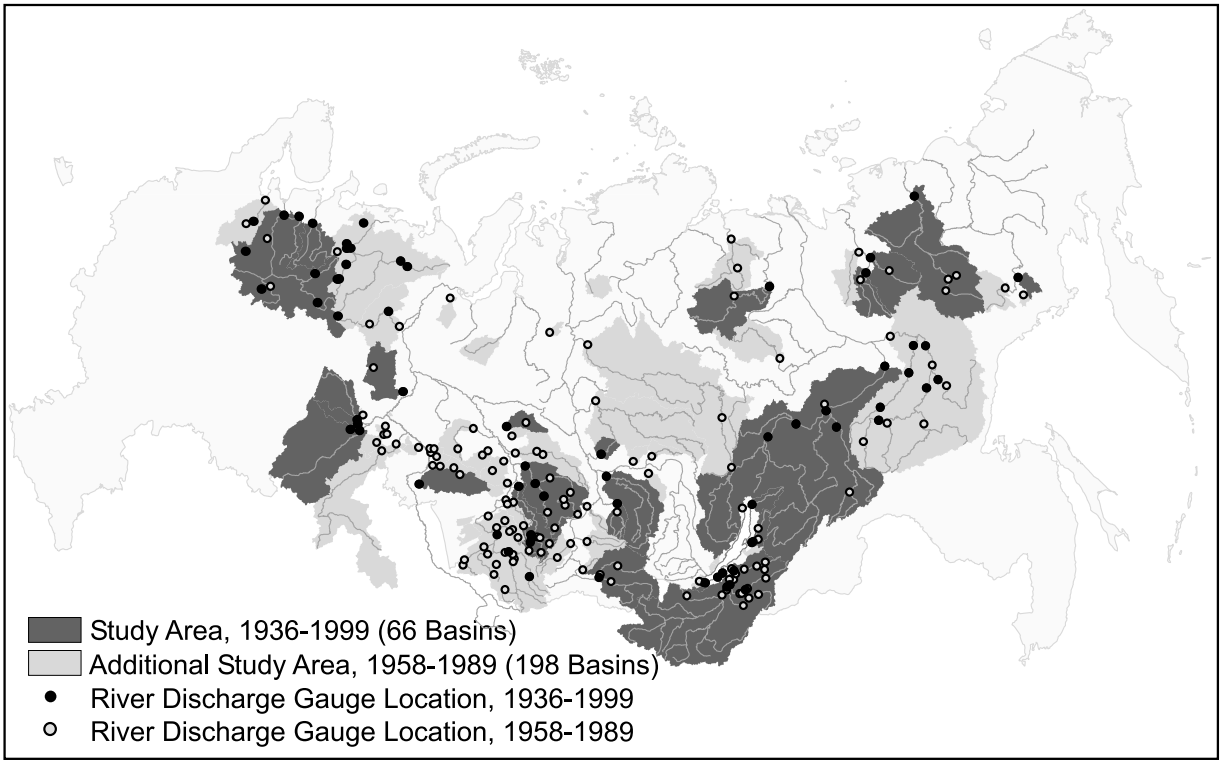

Figure 1. Areas covered by river basins included in the analysis, with those basins used in the 1936–1999 portion of the analysis in dark gray and the additional basins used in the 1958–1989 analysis colored in light gray. Locations of the river discharge gauging stations are plotted as open (1958–1989) and solid (1936–1999) black dots.

delineating their boundaries using available maps and digital elevation models (Section 2.3). Basin sizes range from 151 to 897000 km^2, with a median area of 16500 km^2. As such, they are markedly smaller in area and far more numerous than those examined in previous studies of Eurasian discharge variability [*Berezovskaya et al.* 2004; *Peterson et al.* 2002]. A partial list of basins used in the 1958–1989 analysis is presented in Table 2, and a full description of all basins selected for the 1936–1999 analysis is provided in Table 3.

2.2. Precipitation Data

[9] The four precipitation data sets examined in the first portion of this study are of two types: those interpolated from station data (UW and UDel) and those derived from reanalysis projects (ERA-40 and NCEP) (Table 1). The UDel data set, obtained from the Arctic RIMS project website (http://rims.unh.edu/data.shtml), is interpolated on a 25 km EASE grid and covers the period 1930–2002. The UW data set is based on the UDel data set but is corrected using climatologic and orographic factors in an attempt to more accurately reflect likely precipitation values [*Adam and Lettenmaier*, 2003; *Adam et al.*, 2006; *Hamlet and Lettenmaier*, 2005]. Specifically, additive corrections are applied to account for wetting errors, while multiplicative corrections are used to ameliorate errors associated with orography and gauge undercatch of solid precipitation [*Adam and Lettenmaier*, 2003; *Adam et al.*, 2006]. The UW data set is on a 0.5° geographic grid and includes the years 1930–1989. Later years are not included in the UW data set because of degradation in the quantity and quality of precipitation data after 1990 [*Adam and Lettenmaier*, 2003].

[10] The ERA-40 and NCEP data sets are both derived from reanalysis projects. The ERA-40 data set, obtained on a 2.5° geographic grid, covers the period 1958 to 2002. Monthly values of total precipitation are not readily available for ERA-40, so stratiform (large-scale) precipitation was aggregated with convective precipitation to obtain

Table 1. Summary Statistics for All Four of the Precipitation Data Sets Analyzed[a]

	Resolution	Time Period	Type	Mean P, mm/yr	St. Dev. P, mm/yr	Mean r	Range of r	Mean k
UDel	25 km	1930–2002	Interpolated	453	131	0.61	0.06 to 0.90	0.56
UW	0.5 degree	1930–1989	Interpolated	598	191	0.61	0.11 to 0.88	0.42
ERA-40	2.5 degree	1958–2002	Reanalysis	478	115	0.38	−0.31 to 0.74	0.57
NCEP	~1.9 degree	1948–2005	Reanalysis	771	286	0.39	−0.30 to 0.78	0.35

[a]Includes spatial resolution, time period, method used to create the data set (type), mean annual precipitation across all analysis basins (Mean P), the standard deviation of the mean precipitation (St. Dev. P), the mean Pearson's correlation coefficient with discharge time series (mean r), the range of the precipitation-discharge correlation coefficients (range of r), and the mean runoff ratio (Mean k). There is a substantial contrast in many metrics between the interpolated and reanalysis data sets.

Table 2. Descriptive and Statistical Data on 75 River Basins Used in the 1958–1989 Analysis With Statistically Significant ($p = 0.80$) Trends in River Discharge[a]

Station ID	Name	Lat	Long	DB Area, sq. km	Calc. Area, sq. km	ΔR, %	ΔR, mm/32 yrs	UW ΔP, mm/32 yrs	UDel ΔP, mm/32 yrs	ERA-40 ΔP, mm/32 yrs	NCEP ΔP, mm/yr
5855	Kolyma at Orotuk	62.12	148.47	43600	43390	0.24	46.5		30.9	153.3	26.3
5878	Bokhalcha at Ust'ya	62.10	150.67	13600	13399	0.21	58.4		37.4	125.6	−53.0
6059	Bol'shaya at Pokrovskoye	52.15	107.27	193	164	−1.20	−670.1	−78.9	−67.8	75.5	577.2
6064	Mysovka at Babushkin	51.72	105.87	151	152	−0.11	−68.2			169.1	331.0
6245	Uchur at Chulbu	57.77	130.90	108000	107082	−0.07	−25.1			156.0	−120.4
6250	Allakh-Yun' at Allakh	60.68	135.03	24200	23630	−0.14	−32.2			125.1	
6257	Amga at Terut	62.22	134.13	65400	65287	0.24	23.8		38.3	205.5	−23.4
6295	Dulgalakh at Tomtor	67.12	132.13	23900	23606	−0.15	−20.5			98.6	70.4
6296	Adycha at Ust'-Charky	66.80	136.68	52800	52306	−0.03	−5.2			25.0	115.0
6303	Indigirka at Yurty	64.05	141.88	51100	52163	0.15	21.6	−51.7		84.6	60.9
6404	Barguzin at Mogoito	54.38	110.42	9350	9384	0.34	79.9			144.4	106.2
6411	Selenga at Novoselenginsk	51.10	106.67	360000	363534	−0.12	−7.4	−39.9	−37.8	176.8	−252.6
6412	Selenga at Mostovoy	52.03	107.48	440000	444239	−0.15	−9.3	−41.9	−35.6	186.7	−209.5
6415	Dzhida at Dzhida	50.63	106.12	23300	23628	0.22	20.2	−48.7		176.7	−413.7
6416	Tsakirka	50.70	102.80	1030	1369	−0.22	−41.1		−29.3	265.0	−794.6
6436	Kuitunka at Tarbagatay	51.48	107.37	1060	1144	−1.07	−26.5	−80.6	−53.0		412.5
6445	Kurba at Novaya Kurba	52.05	108.51	5500	5510	−0.05	−6.5	−76.5	−40.6	137.5	224.3
6498	Irkineeva at Bedoba	58.80	97.23	8950	10483	−0.32	−48.2	−138.1	−83.9	280.1	90.4
6500	Taseeva at Mashukovka	57.82	94.32	127000	126034	0.07	13.8			440.6	
6587	Mana at Mansky	55.90	92.50	9260	10973	0.13	44.3		35.2	204.6	124.6
6606	Bol'shoy Pit at Bryanka	59.12	93.48	15100	16337	−0.20	−54.8	−101.0		110.7	43.9
6626	Tunguska at Porog	65.63	90.02	447000	483206	−0.13	−30.0	−87.3	−42.3	155.2	61.3
6657	Ob at Fominskoye	52.45	84.92	98200	98019	−0.15	−51.9	−54.2			−98.6
6658	Ob at Barnaul	53.40	83.82	169000	173890	−0.19	−52.0	−71.5	−38.7		−66.1
6710	Charysh at Ust'-Kumir	51.02	84.32	3480	4048	−0.43	−155.8	−90.0	−52.8		
6715	Charysh at Charishskiy	52.13	83.28	20700	21214	−0.23	−63.9	−115.7	−51.6		−97.0
6722	Aley at Lokot'	51.18	81.20	6450	5600	−0.36	−46.8	−104.6			−184.3
6723	Aley at Rubtsovsk	51.50	81.22	10300	9374	−0.47	−29.9				−149.1
6724	Aley at Aleysk	52.52	82.77	18700	17828	−0.66	−33.9				−125.3
6729	Chumish at Zarinsk	53.73	84.95	15900	16300	−0.23	−48.6	−61.1	−88.4		
6730	Chumish at Tal'menka	53.80	83.57	20600	22513	−0.50	−101.1	−58.4	−84.2	−49.3	
6733	Togool at Togool	53.47	85.92	1200	1225	−0.21	−64.9	−44.4	−75.6	−41.9	143.6
6735	Alambay at Kazantsevo	53.88	85.20	1440	1652	−0.36	−92.4	−36.8	−64.7	−57.6	160.2
6741	Karakan at Rozhdestvenka	54.38	82.45	1140	1255	−0.74	−50.0		−48.7		115.9
6742	Berd' at Maslyanino	54.33	84.23	2480	2523	−0.36	−77.8		−47.8	−69.6	148.7
6751	Inya (Nyzhnyaya) at Kaily	55.32	84.10	15700	15084	−0.34	−25.2		−40.9	−62.4	167.8
6753	Bachat at Bachaty	54.23	86.23	475	729	−0.24	−38.1		−52.0	−90.9	143.6
6756	Oyash at Oyash	55.55	83.87	996	969	−0.50	−45.2				137.9
6757	Tom' at Baliksa	53.43	89.13	2480	2795	−0.14	−70.7				
6760	Tom at Novokuznetsk	53.78	87.15	29800	29983	−0.11	−73.4			−29.8	
6767	Mras-Su at Mysky	53.70	87.80	8790	8767	−0.41	−224.9			39.8	
6770	Kondoma at Kondoma	52.82	87.25	2510	2824	−0.15	−82.8				−149.6
6771	Kondoma at Kuzedeevo	53.33	87.23	7080	6669	−0.18	−92.2				

Table 2. (continued)

Station ID	Name	Lat	Long	DB Area, sq. km	Calc. Area, sq. km	ΔR, %	ΔR, mm/32 yrs	UW ΔP, mm/32 yrs	UDel ΔP, mm/32 yrs	ERA-40 ΔP, mm/32 yrs	NCEP ΔP, mm/yr
6772	Mundybash at Mundybash	53.58	87.30	1060	1121	−0.32	−191.6	−75.6			
6789	Chulym at Balakhta	55.38	91.62	14700	16163	−0.16	−32.8				64.6
6790	Chulym at Krasny Zavod	56.17	89.93	33800	24878	−0.16	−26.4	22.3	26.6		64.6
6795	Bely Iyus at Malaya Siya	54.40	89.45	3520	3588	−0.20	−78.3				
6799	Serezh at Antropovo	55.82	90.15	4580	3169	0.56	36.2		39.6		102.2
6809	Bol'shoy Uluy at Uluy	56.65	90.55	2130	2131	−0.23	−34.6		38.7	80.6	107.7
6849	Ket' at Maksimkin Yar	58.65	86.82	38400	41957	−0.30	−55.7		−84.7	71.6	55.3
6850	Ket' at Rodionovka	58.42	83.67	71500	74249	−0.25	−47.1		−81.4	75.6	
7041	Bol'shoy Aev at Chebaklu	57.10	73.07	4580	5559	0.55	19.8			−64.9	−86.0
7057	Ishim at Ishim	56.10	69.47	140000	212765	0.42	5.0	−60.0	−36.4		−87.4
7058	Ishim at Vikulovo	56.82	70.63	151000	224055	0.53	7.4	−56.9	−33.9		−85.5
7081	Yemets at Kuznetsovo	56.43	68.58	2540	3985	0.45	11.7	−28.8			−132.4
7083	Balakhley at Balakhley	57.13	69.22	2140	1833	1.07	55.5				−107.0
7085	Ashlyk at Ashlyk	57.53	68.68	2080	2798	0.73	52.5				−140.4
7100	Severnaya Sos'va	62.43	60.88	9850	8982	0.22	64.0			53.2	
7105	Severnaya Sosva at Igrim	63.18	64.40	87800	87995	0.11	29.9				
7212	Tura at Tumen'	57.17	65.53	58500	58277	0.39	40.4			47.9	−142.4
7228	Pushma at Bogadinskoe	56.95	65.83	18600	18673	0.54	34.7			27.1	−214.4
7232	Iska at Velizhany	57.55	65.83	895	1280	0.89	66.0				−208.8
7335	Onega at Kazakovo	62.57	39.83	40600	48193	−0.14	−39.4			192.7	
7371	Yug at Podosinovets	60.27	47.07	15200	19213	0.13	29.3	59.0	84.2	153.7	116.2
7381	Luza at Krasavino	60.72	47.60	16300	16688	0.26	59.5	36.7	71.8	154.4	
7387	Vuchegda at Kuzhba	61.77	53.67	26500	36275	0.08	22.5		65.6	69.7	65.0
7481	Pechora at Yaksha	61.82	56.85	9620	9268	−0.11	−56.1		50.0		
7510	Izhma at Ust'-Ukhta	63.62	53.90	15000	13408	0.09	27.2		23.9	90.3	
7518	Pizhma at Levkinskaya	64.77	51.10	2250	2347	−0.21	−62.1			86.1	−52.7
7519	Pizhma at Borovaya	65.27	51.85	4890	4865	−0.13	−37.7			86.1	−60.0
7521	Tsil'ma at Trusovo	65.47	51.37	20900	19364	−0.15	−50.7			43.2	−125.7
7566	Onega at Porog	63.82	38.47	55700	64420	−0.10	−27.9			175.1	68.2
7567	Mezen'	65.00	45.62	56400	56703	−0.14	−48.1			91.3	−60.4
7568	Pechora at Ust'-Tsilma	65.42	52.28	248000	242077	−0.07	−31.2			80.9	

[a]In addition to the R-ArcticNet 3.0 station identifier (Station ID), station name (Name), latitude (Lat), and Longitude (Lon), the table includes the published area of each basin (DB Area) as well as the area calculated from our basin polygons (Calc. Area). Statistically significant trends in river discharge (percent and mm/32 yrs) and all four precipitation (mm/32 yrs) data sets are also included.

values for total precipitation. The NCEP data set begins in 1948 and continues to the present, with a spatial resolution of approximately 1.9°. We recognize the uncertainty inherent in utilizing reanalysis-based precipitation time series in the Arctic and include them here because they have been widely utilized in the literature [e.g., *Serreze et al.*, 2002; *Berezovskaya et al.*, 2004].

[11] For each of the four precipitation data sets, we derive total annual precipitation by clipping each precipitation grid with the delineated basin map (Section 2.3). Any grid cell falling partially or entirely within a river basin is included in the analysis for that basin, and a grid cell may be aggregated into more than one basin if appropriate. All data values for each basin are summed and divided by the number of included cells to calculate mean total annual precipitation for each basin. We recognize the possibility that variations in grid cell size among the precipitation data sets could influence our ability to detect relationships between discharge and precipitation, particularly in the smallest river basins. However, no statistically significant relationship ($p = 0.10$) was observed between discharge-precipitation correlation coefficients and basin area for any of the four data sets,

Table 3. Descriptive and Statistical Data on All 66 River Basins Used in the 1936–1999 Analysis[a]

Station ID	Name	Lat	Long	r	A, sq. km	ΔR, %	ΔR, mm/ 64 yrs	ΔP, mm/ 64 yrs	k	*R*	ΔP/ ΔR
5878	Bokhalcha	62.1	150.67	0.64	13,600	0.06	16.18	24.69	0.88		
6062	Rechka at Posol'skoye	51.95	106.35	0.68	565	−0.04	−27.90	**−133.82**	1.90		
6064	Mysovka at Babushkin	51.72	105.87	0.42	151	**−0.18**	**−107.08**	−42.84	1.15	0.46	0.40
6145	Lena at Krestovskoe	59.73	113.17	0.79	440,000	**0.09**	**26.28**	−10.25	0.80	−0.31	−0.39
6146	Lena at Solyanka	60.48	120.7	0.79	770,000	**0.17**	**46.77**	−2.70	0.73	−0.04	−0.06
6147	Lena at Tabaga	61.83	129.6	0.82	897,000	**0.11**	**27.03**	3.47	0.67	0.09	0.13
6210	Bol'shoy Patom at Patoma	60.17	116.8	0.66	27,600	−0.01	−2.58	**27.62**	1.13		
6216	Olekma at Kudu-Kel'	59.37	121.32	0.84	115,000	**0.18**	**49.83**	***9.81***	0.63	0.12	0.20
6232	Aldan at Tommot	58.97	126.27	0.71	49,500	**0.11**	**37.69**	***47.96***	0.61	0.78	1.27
6234	Aldan at Ust'-Mil'	59.63	133.03	0.72	269,000	**0.12**	**37.97**	18.16	0.65	0.31	0.48
6235	Aldan at Okhotskiy Perevoz	61.87	135.5	0.74	514,000	*0.08*	***20.72***	6.27	0.58	0.18	0.30
6247	Maya at Chabda	59.78	134.75	0.65	165,000	−0.04	−8.69	−4.25	0.50		
6255	Amga at Buyaga	59.67	127.05	0.69	23,900	0.10	15.80	**45.16**	0.35		
6256	Amga at Amga	60.9	131.98	0.62	56,800	**0.27**	**25.43**	23.68	0.26	0.24	0.93
6257	Amga at Terut	62.22	134.13	0.52	65,400	**0.32**	**29.08**	***28.93***	0.25	0.25	0.99
6292	Olenek at Sukhona	68.62	118.33	0.69	127,000	**0.27**	**46.15**	***−21.13***	0.62	−0.28	−0.46
6293	Yana at Verkhoyansk	67.34	133.38	0.71	45,300	0.10	10.12	−4.37	0.44		
6298	Adycha at Yurduk-Kumakh	68.02	135.27	0.47	89,600	*0.21*	***35.47***	**−41.17**	0.83	−0.96	−1.16
6353	Indigirka at Vorontsovo	69.57	147.53	0.56	305,000	0.12	18.64	**−36.24**	0.71		
6402	Verkhnyaya Angara at Zaimka	55.85	110.15	0.52	20,600	*0.07*	***23.61***	13.93	1.28	0.76	0.59
6405	Barguzin at Barguzin	53.6	109.6	0.64	19,800	−0.04	−7.33	6.28	0.56		
6411	Selenga at Novoselenginsk	51.1	106.67	0.76	360,000	*0.13*	***7.82***	−10.67	0.21	−0.29	−1.36
6412	Selenga at Raz'ezd Mostovoy	52.03	107.48	0.77	440,000	0.04	2.85	−13.69	0.21		
6428	Khilok at Maleta	50.83	108.4	0.62	25,700	−0.09	−7.41	−14.99	0.25		
6430	Khilok at Khailastuy	51.2	106.97	0.67	38,300	**−0.23**	**−17.36**	***−23.04***	0.23	0.31	1.33
6448	Snezhnaya at Vydrino	51.43	104.63	0.75	3000	*−0.15*	***−72.92***	***−39.37***	0.73	0.39	0.54
6500	Taseeva at Mashukovka	57.82	94.32	0.73	127,000	−0.06	−10.63	***−31.03***	0.46		
6537	Yenisey at Kyizyil	51.72	94.4	0.49	115,000	*−0.08*	***−21.39***	**−75.89**	0.61	2.15	3.55
6594	Kan at Kansk	56.22	95.7	0.61	23,000	−0.06	−18.74	***−29.45***	0.84		
6606	Bol'shoy Pit at Bryanka	59.12	93.48	0.63	15,100	−0.06	−16.71	**−53.83**	0.55		
6658	Ob at Barnaul	53.4	83.82	0.76	169,000	−0.06	−16.03	0.21	0.56		
6670	Biya at Biysk	52.55	85.28	0.78	36,900	−0.08	−34.29	−23.99	0.81		
6679	Chulyshman at Balukhcha	51.28	87.72	0.75	16,600	*0.09*	***26.98***	−12.74	0.93	−0.44	−0.47
6760	Tom at Novokuznetsk	53.78	87.15	0.78	29,800	*−0.11*	***−77.52***	**−68.32**	0.94	0.83	0.88
6762	Tom' at Tomsk	56.5	84.92	0.70	57,000	−0.07	−37.12	**−58.38**	0.92		
6771	Kondoma at Kuzedeevo	53.33	87.23	0.75	7080	**−0.23**	**−124.33**	**−80.90**	0.65	0.42	0.65
6772	Mundybash at Mundybash	53.58	87.3	0.71	1060	**−0.31**	**−189.16**	**−87.98**	0.74	0.34	0.47
6792	Chulym at Zyryanskoye	56.85	86.62	0.34	92,500	−0.02	−2.80	***−34.51***	0.43		
6794	Chulym at Baturino	57.78	85.15	0.47	131,000	0.01	2.43	−15.79	0.42		
6816	Kiya at Marizhinsk	56.2	87.78	0.39	9820	−0.01	−5.37	−17.46	0.99		
6866	Tim at Napas	59.85	81.95	0.50	24,500	*0.11*	***25.58***	***18.37***	0.52	0.37	0.72
7011	Om' at Kalachinsk	55.07	74.58	0.31	47,800	−0.41	−14.10	−21.95	0.09		
7093	Konda at Bol'chary	59.82	68.8	0.44	65,400	**0.43**	**61.08**	***28.09***	0.32	0.15	0.46
7103	Severnaya Sosva at Sosva	63.65	62.1	0.78	65,200	*0.07*	***19.21***	***34.88***	0.57	1.04	1.82
7154	Tobol at Yalotorovsk	56.67	66.35	0.46	241,000	−0.00	−0.08	21.83	0.04		
7185	Iset' at Isetskoye	56.48	65.35	0.46	56,000	0.12	4.61	13.54	0.09		
7212	Tura at Tumen'	57.17	65.53	0.52	58,500	**0.45**	**52.01**	***40.55***	0.25	0.20	0.78
7228	Pushma at Bogadinskoe	56.95	65.83	0.48	18,600	**0.50**	**34.82**	***39.69***	0.15	0.18	1.14
7335	Onega at Kazakovo	62.57	39.83	0.65	40,600	**0.19**	**52.36**	**76.16**	0.46	0.67	1.45
7371	Yug at Podosinovets	60.27	47.07	0.74	15,200	**0.15**	**36.90**	**42.25**	0.46	0.53	1.15
7387	Vuchegda at Malaya Kuzhba	61.77	53.67	0.73	26,500	**0.28**	**80.35**	**147.26**	0.50	0.91	1.83
7407	Vim at Veslyana	62.98	50.88	0.70	19,100	0.06	20.01	***32.97***	0.57		

Table 3. (continued)

Station ID	Name	Lat	Long	r	A, sq. km	ΔR, %	ΔR, mm/ 64 yrs	ΔP, mm/ 64 yrs	k	*R*	ΔP/ ΔR
7421	Vaga at Philyaevskaya	61.12	42.18	0.70	13,200	0.05	12.01	10.62	0.47		
7443	Pinega at Kulogory	64.72	43.48	0.67	36,700	**0.20**	**62.57**	5.65	0.57	0.05	0.09
7481	Pechora at Yaksha	61.82	56.85	0.75	9620	**0.13**	**62.83**	**127.38**	0.90	1.83	2.03
7497	Usa at Petrun'	66.47	60.73	0.55	27,500	**0.18**	**104.26**	**54.680**	1.43	0.75	0.52
7498	Usa at Adzva-Vom	66.55	59.42	0.61	54,700	**0.11**	**55.72**	**75.80**	1.19	1.62	1.36
7510	Izhma at Ust'-Ukhta	63.62	53.9	0.64	15,000	**0.18**	**56.07**	**99.74**	0.52	0.93	1.78
7511	Izhma at Kartaiol	64.53	53.33	0.74	22,700	**0.17**	**49.83**	**72.16**	0.50	0.72	1.45
7515	Ukhta at Ukhta	63.55	53.72	0.51	4290	**−0.09**	**−28.21**	**65.31**	0.57	−1.32	−2.32
7519	Pizhma at Borovaya	65.27	51.85	0.60	4890	*0.09*	***24.89***	***−32.88***	0.55	−0.73	−1.32
7521	Tsil'ma at Trusovo	65.47	51.37	0.66	20,900	0.02	7.49	***−38.56***	0.66		
7524	Sula at Kotkina	67.03	51.13	0.56	8500	**0.11**	**36.61**	**−69.73**	0.78	−1.49	−1.90
7564	Severnaya Dvina at Pinega	64.13	41.92	0.51	348,000	**0.10**	**27.52**	***24.94***	0.51	0.46	0.91
7567	Mezen' at Malonisogorskaya	65	45.62	0.74	56,400	0.04	12.49	10.36	0.64		
7568	Pechora at Ust'-Tsilma	65.42	52.28	0.67	248,000	**0.09**	**37.21**	**87.45**	0.83	1.95	2.35

[a]Statistically significant trends in discharge (ΔR) and precipitation (ΔP) are marked with italics ($p = 0.80$) and boldface ($p = 0.90$). Also included are correlation coefficients between precipitation and discharge time series (r), basin area (A), runoff ratio (k), and values of R_p and ΔP/ΔR for those basins in which discharge trends are statistically significant at the $p = 0.80$ level or above.

suggesting that differences in grid cell size are unlikely to bias the calculation of discharge-precipitation relationships in small basins. Additionally, we performed a sensitivity analysis on three representative basins to determine the impact of varying spatial resolution, aggregating 0.5° UW data to match the grid size and spacing of 2.5° ERA-40 data. We then compared mean annual precipitation and discharge-precipitation correlation between the two resolutions. The greatest change in mean annual precipitation was 3.15%, while the largest difference in the Pearson's correlation coefficient calculated between annual discharge and precipitation was 0.06. These small resolution-dependant changes suggest that variations in resolution of precipitation data sets have minimal impact on this analysis.

2.3. Basin Delineation

[12] For each of the 198 river gauging stations identified in section 2.1, the Hydro1K One Kilometer Digital Elevation Model (http://edcdaac.usgs.gov/gtopo30/hydro/index.asp) was used to derive an initial map of basin boundaries, which was then corrected using the Digital Chart of the World (DCW) global hydrology data set (http://www.maproom.psu.edu/dcw/). To produce the initial map, the R-ArcticNet station locations were used as pour points in combination with a flow accumulation grid computed from the Hydro1K DEM using ESRI ArcGIS 9.0. Because the precision of station locations in the R-ArcticNet 3.0 database is available to only 0.01 degrees, mapping of their coordinates can place the station some distance from the actual river channel. When a station location was initially placed outside the river channel, it was manually moved to the nearest location on the river channel for which the calculated and R-ArcticNet 3.0 basin areas differed by no more than 20%. Most such shifts involved differences of less than 10 km between the initial location and the corrected location. More than 80% of the calculated basin areas match the R-ArcticNet database values to within +/−20%. Most of the basins outside of this range are small or are in very flat areas where precise basin delineation is difficult.

2.4. Intercomparison of Precipitation Data Sets, 1958–1989 (198 Basins)

[13] We utilize annual river discharge to evaluate the four precipitation data sets for three reasons. First, past research suggests that interannual variability in runoff is closely related to associated precipitation anomalies, with near perfect covariance observed in humid basins and somewhat lower values observed in more arid catchments [*Milly and Dunne*, 2002]. Second, the discharge data provides an opportunity for completely independent validation that is otherwise unavailable from a simple comparison among precipitation data sets. Finally, the uncertainties in the precipitation data sets are much larger than those in the discharge data. While errors in precipitation data sets can range as high as 50–100%, errors in annual river discharge values are ∼2–5% for rivers without floodplains and ∼5–12% for rivers with floodplains [*Lammers et al.*, 2001].

[14] We use four different methods to contrast the four precipitation data sets, including (1) comparison of mean annual discharge and precipitation values, (2) correlation of discharge and precipitation time series, and (3) comparison of precipitation and discharge linear regression trends. In addition, we derive runoff coefficients (k) for each basin by calculating the mean ratio of annual discharge to annual precipitation over the period of study. In combination with discharge and precipitation trends, the runoff coefficients are used to calculate R_p, a new metric denoting the percentage of observed discharge trend over the period of observation that is contributed by the observed precipitation trend.

[15] The Pearson's product-moment correlation coefficient is calculated between the 1958–1989 precipitation and discharge time series for each of the 198 basins. When comparing the correlation coefficients among the basins, the large sample size allows us to use statistical approaches unavailable in studies utilizing a smaller number of catchments. While we recognize the limitations of the Pearson's correlation coefficient, particularly its sensitivity to outliers and its inability to detect multiplicative

shifts in time series [*Legates and McCabe*, 1999], we choose to use it here for two reasons. First, correlation coefficients are widely used in examinations of precipitation and discharge [e.g., *Berezovskaya et al.*, 2004; *Yin et al.*, 2004; *Kattsov and Walsh*, 2000]. Second, they are easily interpretable by a large segment of the scientific community, unlike alternative such as the coefficient of agreement (*E*) and the index of agreement (*d*) [*Legates and McCabe*, 1999]. To address some of the limitations inherent in the Pearson's correlation coefficient, we also use other metrics such as differences in mean annual precipitation to examine multiplicative differences between data sets. When necessary, we use the median rather than the mean as a measure of centrality in order to reduce the influence of outliers in some portions of the analysis.

[16] Long-term trends in the precipitation and discharge time series are calculated using least squares linear regression analysis. Statistical significance is determined using the Mann-Kendall test for monotonic trend [*Mann*, 1945; *Kendall*, 1975; *Maidment*, 1993], a rank-based, nonparametric test for monotonic trend. A nonparametric test was preferred over a parametric test to avoid potential problems introduced by data skew. Mann-Kendall is commonly used to detect long-term trends in hydrologic time series [e.g., *Hirsch et al.*, 1991; *Burn*, 1994; *Lins and Slack*, 1999; *Smith*, 2000; *Hodgkins et al.*, 2005].

[17] For each basin with trends in both precipitation and discharge statistically significant at the $p = 0.80$ level, we calculate a dimensionless metric (R_p) that denotes the percentage of observed discharge trend over the period of observation that is contributed by the precipitation trend:

$$R_p = \Delta P/(\Delta R/k)$$

Where ΔP is the precipitation trend in mm/yr over the period of study, ΔR is the trend in discharge in mm/yr, and k is the long-term mean runoff ratio calculated using the precipitation data set in question. Differences in the distribution of R_p among the precipitation data sets allow us to evaluate the utility of each in explaining discharge variability, with high values ($R_p > 0.5$) indicating a large proportion of discharge trend explained by precipitation trend and negative values ($R_p < 0$) indicating opposing trends in discharge and precipitation.

[18] We include k in the formulation of R_p because an increase or decrease in precipitation can result in a discharge trend of lesser magnitude because of the effect of evapotranspiration (ET). The proportion of the precipitation trend expressed in the discharge trend is related to whether ET is water limited or energy limited. If actual ET equals potential ET in a river basin, then any increase in precipitation will be partitioned into increased runoff. If, however, potential ET is greater than actual ET, then some portion of any increase in precipitation will result in greater ET. As such, given an increase in precipitation, a high-ET basin such as those in the southern Ob' region is likely to experience a smaller increase in discharge, while a low-ET basin is likely to experience an increase in discharge of a similar magnitude to the increase in precipitation. It is probable that k will change with time, and recent studies have shown increasing runoff ratios in many areas of northern Eurasia [*Rawlins et al.*, 2006]. As such, R_p should be treated as an approximation. For the purposes of calculating R_p, we assume that on annual timescales the storage term in the water balance equation is constant, though it is in fact possible that changes in storage contribute to increasing or decreasing runoff. This assumption also contributes to uncertainty in R_p.

[19] There are certainly spatial variations in how ET is limited, but our understanding of these variations is constrained by a lack of reliable ET data. Therefore in addition to R_p, we calculate $\Delta P/\Delta R$, which eliminates k from R_p and assumes that any trend in precipitation will be reflected directly in a runoff trend and that ET rates will stay constant with increased precipitation. Recently observed increases in runoff ratios for northern Eurasia suggest that the majority of observed precipitation changes are reflected in runoff, pointing toward $\Delta P/\Delta R$ as a preferable metric [*Rawlins et al.*, 2006]. However, it is probable that for many basins, the actual proportion of the discharge trend associated with the precipitation trend lies somewhere between the end-member cases of R_p and $\Delta P/\Delta R$.

2.5. Role of Precipitation in Observed Discharge Increases, 1936–1999

[20] While all four precipitation data sets cover the period 1958 to 1989, only the UDel data set is available from 1936 to 1999, the period over which *Peterson et al.* [2002] identify a 7% increase in Eurasian runoff. Therefore we are able to use only the UDel data set to test the hypothesis that precipitation increases play a large role in driving observed positive discharge trends. As before, we use the Mann-Kendall test to examine long-term covariance between precipitation and discharge. We compute 1936–1999 trends for discharge and precipitation, and basin runoff ratios calculated over the same period are used to derive R_p and $\Delta P/\Delta R$ for all basins with statistically significant trends in discharge ($p = 0.80$). The spatial and statistical distributions of R_p are used to estimate the effect of precipitation trends on observed changes in discharge.

[21] Finally, we examine the possibility that permafrost thaw or other associated processes have contributed to observed annual river discharge increases. Presumably, if runoff increases are related to permafrost thaw [*Oelke et al.*, 2004], some correlation should exist between annual discharge trend and the amount and/or state of permafrost. For each basin, we calculate the total extent of ground ice using the global permafrost map compiled by *Brown et al.* [1998]. The map contains four classes of permafrost extent: continuous (90–100% coverage), discontinuous (50–90%), sporadic (10–50%), and isolated (0–10%). Additionally, each category of permafrost extent is divided into high ice richness (>20%), medium ice richness (10–20%), and low ice richness (<10%). We calculate the area covered by each of the 12 possible classes in each basin and, utilizing the median percent permafrost cover (95%, 70%, 30%, and 5%, respectively) and mean ground ice content within each class (25%, 15%, and 5%), calculate the proportion of ground ice in the basin as a whole. In those basins displaying statistically significant runoff trend ($p = 0.80$, n = 40), we then compare the proportion of ground ice with annual discharge trend to assess any correlation. In addition, we use a Student's T-test to detect any statistically significant differ-

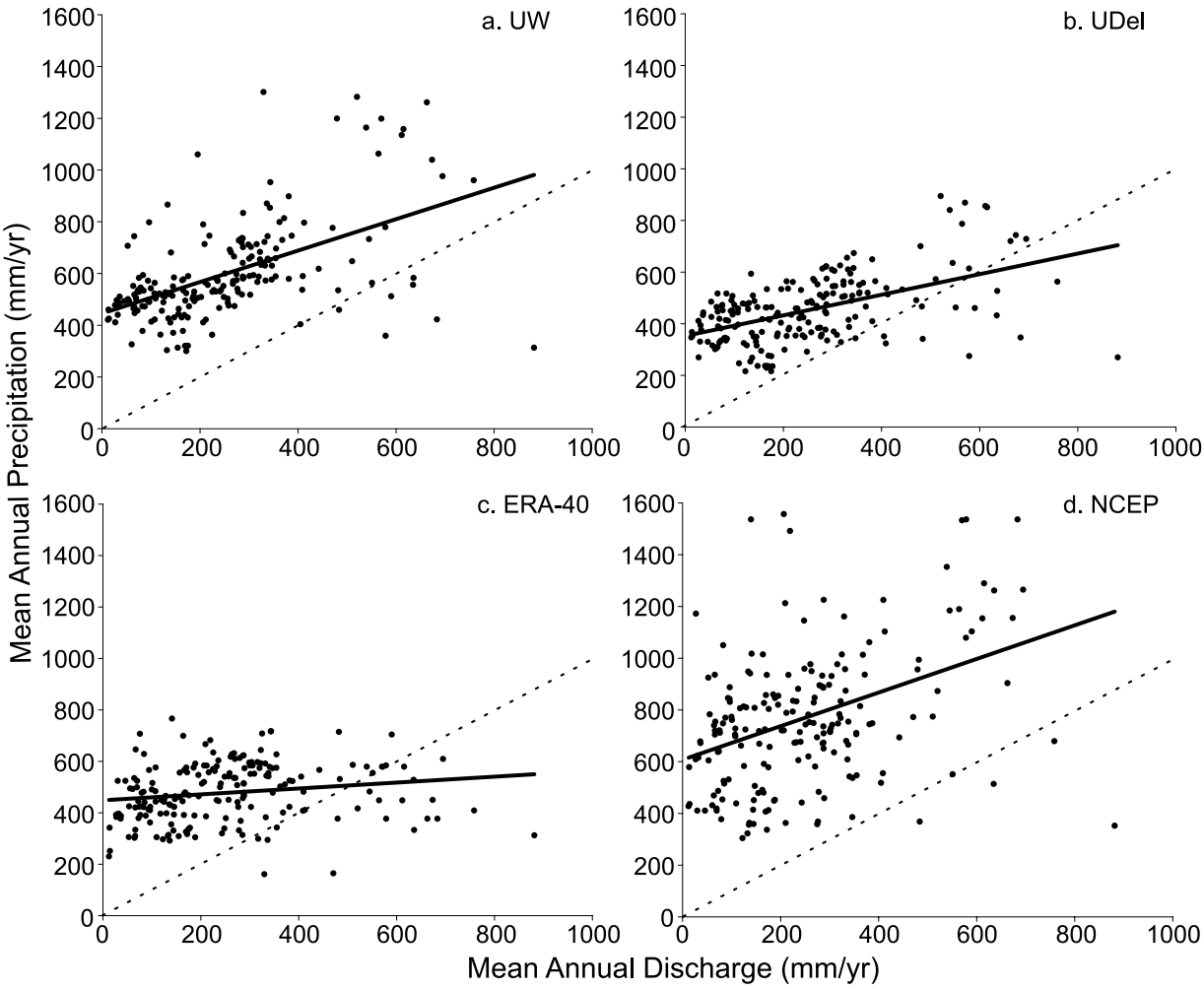

Figure 2. Mean annual discharge and mean annual precipitation for the (a) UW, (b) UDel, (c) ERA-40, and (d) NCEP data sets in 198 basins. Note the substantial difference in slope between ERA-40 trend line and those of the other data sets as well as the higher values characteristic of the NCEP data set.

ence in the mean value of R_p between basins with less than 1% ground ice versus basins with more than 4%.

3. Results

3.1. Comparison of Precipitation Data Sets, 1958–1989

[22] Mean annual values for discharge and precipitation between 1958 and 1989 are shown in Figures 2a–2d for all 198 river basins. All correlations are generally low, as would be expected given the wide range of basin sizes and uncertainties in the precipitation data. However, NCEP precipitation values are markedly higher than UW values, which in turn are higher than UDel and ERA-40 values. The higher mean precipitation values in the UW and NCEP data sets are highlighted in Table 1, where the mean k values for UW and NCEP (0.42 and 0.35, respectively) are substantially lower than are the mean runoff ratios derived from the UDel and ERA-40 data sets (0.56 and 0.57). NCEP and particularly ERA-40 mean precipitation are substantially less correlated ($r = 0.39$ and $r = 0.21$, respectively) with mean discharge than are UW and UDel ($r = 0.49$ and $r = 0.51$, respectively). In addition, the expected positive relationship between mean annual precipitation and discharge visible in the UDel, NCEP, and UW trend lines in Figure 2 is notably weaker in ERA-40 data.

[23] Table 4 presents mean correlation coefficients among the four precipitation data products as well as between each precipitation data set and river discharge for all 198 basins. The high correlation between UDel and UW data sets was anticipated, as additive and multiplicative corrections made by *Adam and Lettenmaier* [2003] to the UDel data set result in few changes in the pattern of interannual variability. NCEP and ERA-40 precipitation are less correlated with the interpolated UDel and UW data sets and with each other. Figures 3a–3c show maps of correlation between UW, ERA-40, and NCEP time series for all 198 river basins. The UW-UDel map is not shown because all correlation coefficients are very high, while the ERA-40-UDel and NCEP-UDel correlation maps are nearly identical to Figures 3a and 3b, respectively. All of the data sets are well correlated in European Russia and also parts of Eastern Siberia. In Central Siberia, however, NCEP and especially ERA-40 precipitation differ markedly from the UW data set. ERA-40 and NCEP are more correlated in this region but disagree in parts of Eastern Siberia and southward of Lake Baikal.

Table 4. Mean Pearson's Correlation Coefficients Among the Basin-Averaged Precipitation Time Series As Well As Between Each Precipitation Data Set and the Discharge Data (n = 198 Basins)

	UW	UDel	ERA-40	NCEP	Discharge
UW	1	0.95	0.43	0.53	0.61
UDel	0.95	1	0.46	0.54	0.6
ERA-40	0.43	0.46	1	0.44	0.38
NCEP	0.53	0.54	0.44	1	0.39
Discharge	0.61	0.60	0.38	0.39	1

[24] Table 4 also includes mean correlation coefficients between time series of the four precipitation data sets and river discharge (n = 198). Both the UDel and UW data sets are moderately correlated (r = 0.60 and r = 0.61 respectively) with discharge, while the ERA-40 and NCEP data sets are less so (r = 0.38 and r = 0.39 respectively). Figures 4a–4d show correlation coefficients between precipitation and discharge for each of the four data sets. As above, the UDel and UW data sets are very similar, showing high correlation in most areas except in portions of the Ob' basin. Decorrelation in this region may be related to irrigation withdrawals for large-scale agricultural production in the area [*Yang et al.*, 2004a]. Consistently lower correlation with discharge is found for ERA-40 than for the interpolated precipitation data sets (Figure 4c), though it is still relatively high for European Russia, Eastern Siberia, and portions of the Ob' Basin. Similar to the pattern of correlation with interpolated precipitation data sets (Figure 3b), ERA-40 displays low correlation with discharge in portions of Northeastern Siberia and in large parts of Central Siberia. On the whole, the interpolated UDel and UW data sets correlate more strongly with discharge than do either of the reanalysis data sets.

[25] A second way to evaluate the four precipitation data sets is to examine the agreement or disagreement between statistically significant long-term trends in discharge and precipitation (1958–1989). Table 2 presents trends in discharge and precipitation for those basins with statistically significant trends in discharge and one or more precipitation data set. The mean discharge trend over this period is −1%, with a maximum trend of 120% and a minimum trend of −107%. Figures 5a–5d show those basins with either positive or negative trend (p = 0.80) for all four precipitation data sets. Figure 6 shows the same for discharge. The trends in discharge and UW precipitation (Figure 5a) have relatively similar spatial patterns, with 21 basins in which statistically significant discharge and precipitation trends agree and 6 in which the trends oppose. The same is true for the UDel data set (Figure 5b), with 30 basins in agreement and 5 opposed. In contrast, ERA-40 precipitation diverges dramatically from discharge (Figure 5c), with precipitation increases observed nearly everywhere in the Eurasian Arctic except the Southern Ob' basin. Unlike for the interpolated UW and UDel precipitation data sets, the ERA-40 trends are often opposite to discharge trends, with 22 basins having trends that agree in sign and 25 opposed. The same is true for the NCEP data set (Figure 5d), with 23 basins in agreement and 32 in opposition. Unlike the ERA-40 data set, the NCEP data set does not show dramatic increases in precipitation across Northern Eurasia, although it also does not show much similarity to the spatial patterns in runoff visible in Figure 6. Only four river basins have statistically significant trends in discharge without a corresponding trend in at least one of the four precipitation data sets, which supports our hypothesis that precipitation change acts as a significant driver of discharge trend.

[26] Figures 7a–7d plots statistically significant trends (mm/32 yrs) in precipitation and discharge for each data set. The UDel precipitation trends have the highest coefficient of determination with discharge trend (R^2 = 0.49), followed by UW (R^2 = 0.22). The ERA-40 (R^2 = 0.09) and NCEP (R^2 = 0.02) coefficients of determination are so small that any observed relationship is probably meaningless. The UW and UDel data sets show the anticipated positive relationship between discharge and precipitation trends, which complements our finding above that for these two data sets discharge and precipitation trends tend to agree in sign.

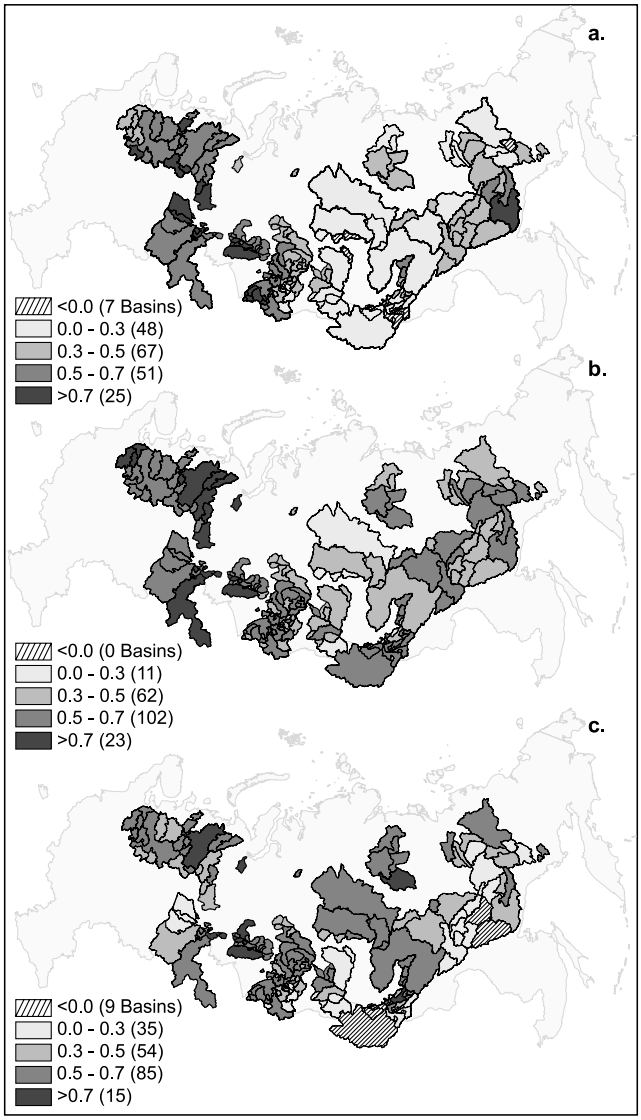

Figure 3. Pearson's correlation coefficients between (a) UW and ERA-40, (b) UW and NCEP, and (c) ERA-40 and NCEP time series for all 198 study basins. ERA-40 time series diverge substantially from the UW data over much of Central Siberia, while the NCEP and ERA time series diverge in parts of Eastern Siberia.

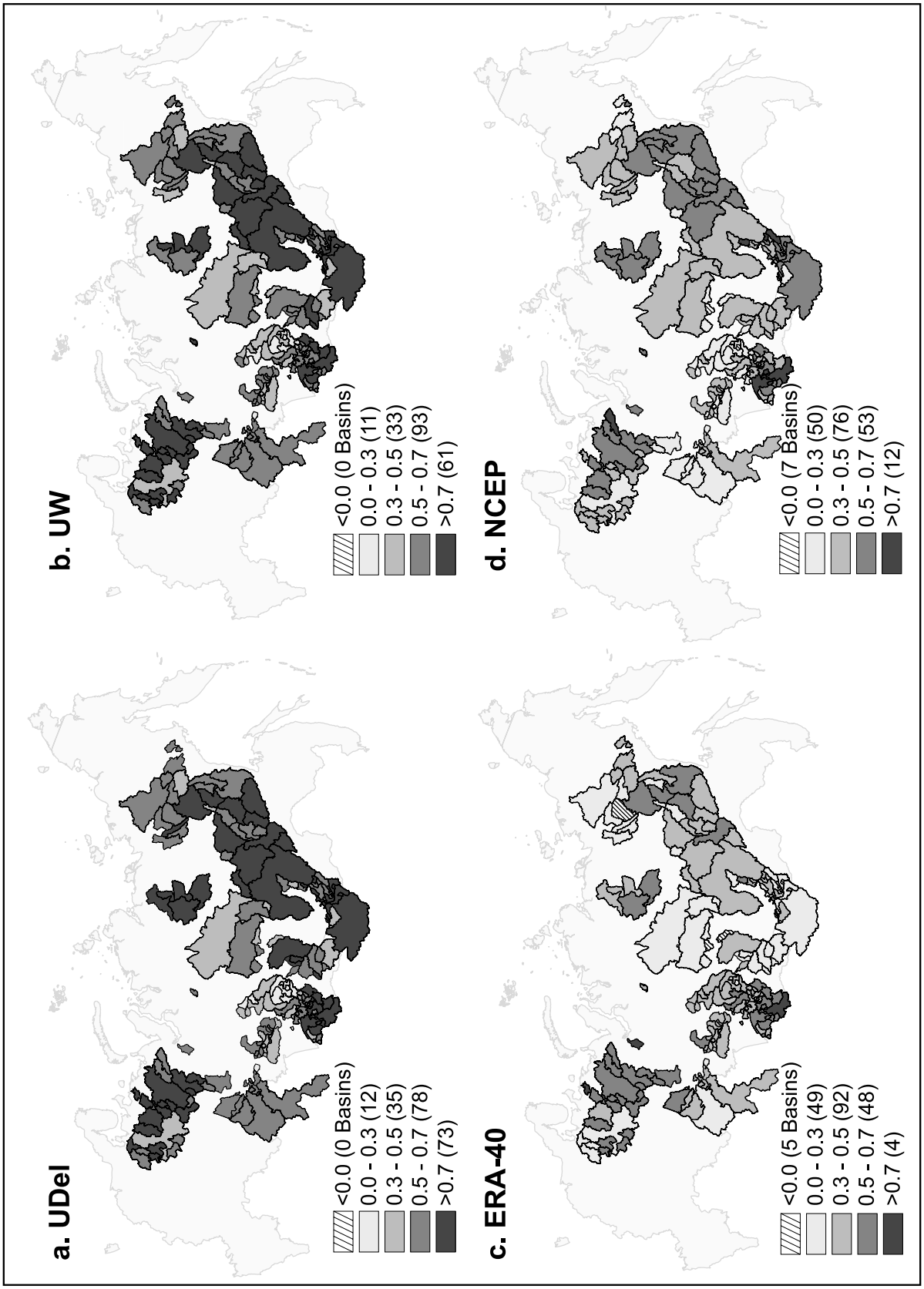

Figure 4. Pearson's correlation coefficients between discharge time series and the (a) UDel, (b) UW, (c) ERA-40, and (d) NCEP data sets. Note the similarities between the UDel and UW data as well as the substantially lower correlation between discharge and the ERA-40 and NCEP products.

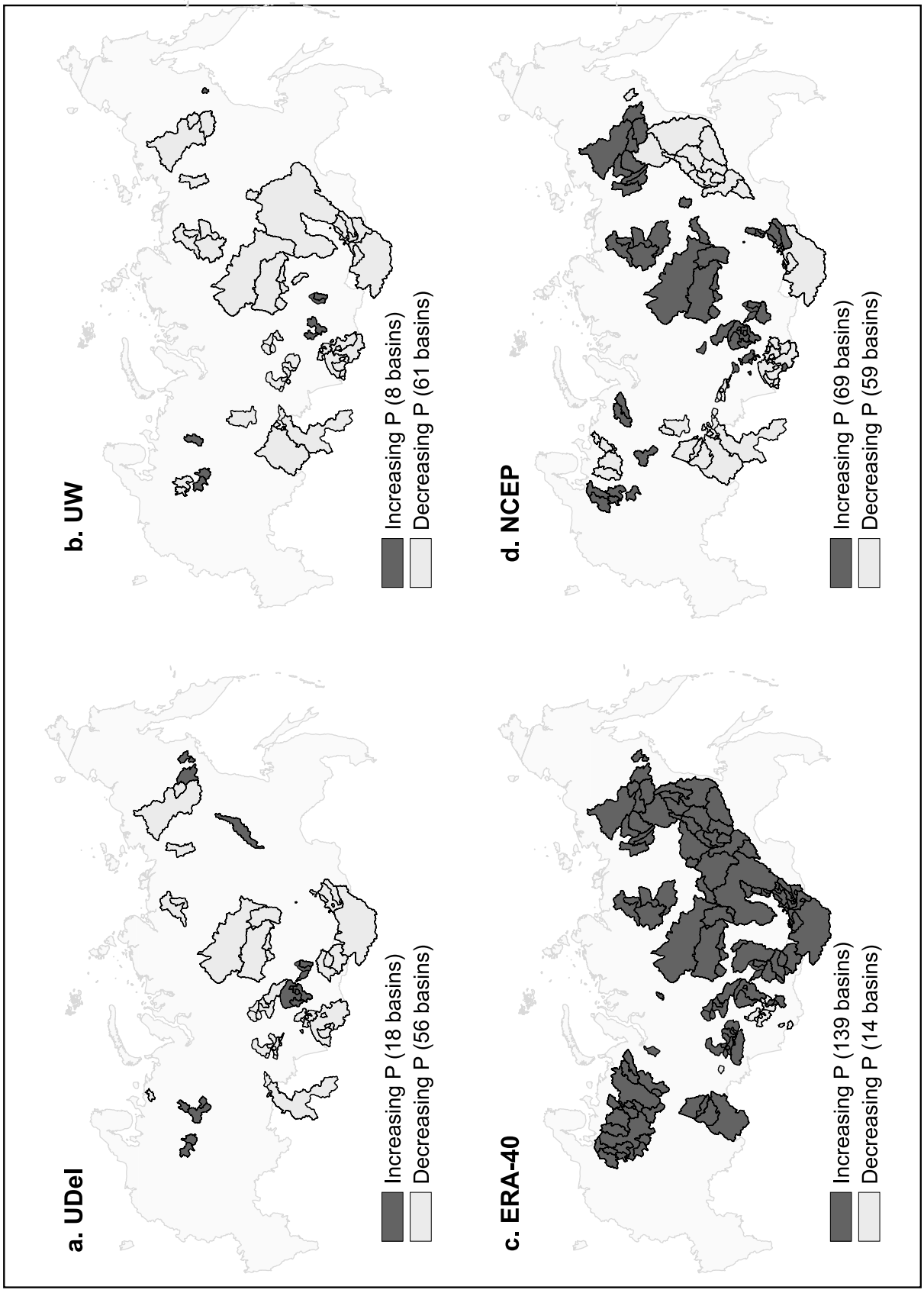

Figure 5. Basins with statistically significant ($p = 0.80$) trends (increasing or decreasing) in precipitation for the (a) UDel, (b) UW, (c) ERA-40, and (d) NCEP data sets. Widespread increasing trends in the ERA-40 data are shown as well as agreement between trends in the UDel and UW data sets.

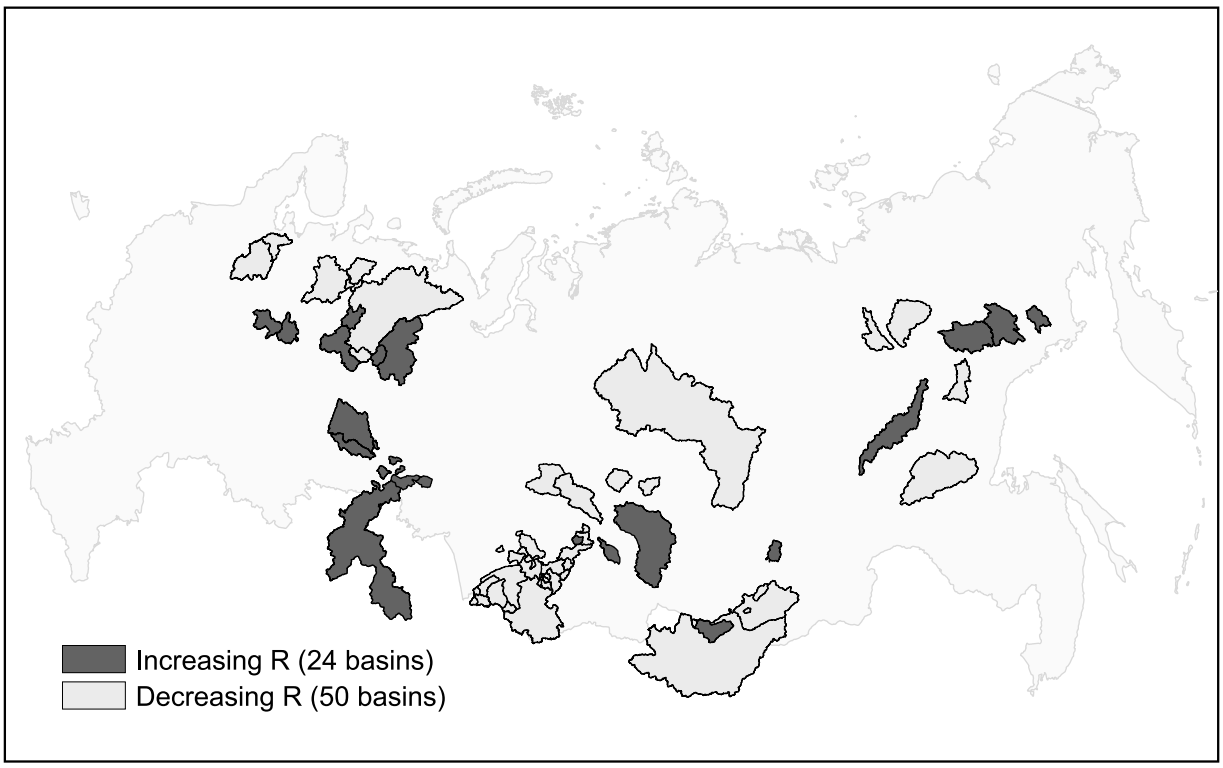

Figure 6. Basins with statistically significant (p = 0.80) trends (increasing or decreasing) in river discharge. Comparison with Figure 5 reveals substantial agreement with trends in the UDel and UW precipitation data sets and marked divergence from the NCEP and ERA-40 products.

[27] In order to examine the proportion of the observed discharge trend that could be explained by the trend in precipitation, we calculated the metrics R_p and $\Delta P/\Delta R$ as described in Section 2.4 for each basin with statistically significant trends in precipitation and discharge. Figure 8 shows the cumulative percentage of basins with values of R_p greater than several thresholds. A value of 1 indicates that the precipitation trend in question could account for 100% of the observed discharge trend, while negative values indicate that the precipitation and discharge trends are in opposing directions. The median of R_p is 0.42 for both the UDel and UW data sets, −0.08 for the ERA-40 data set, and −0.26 for the NCEP data set. Meanwhile, the median values of $\Delta P/\Delta R$ for the Udel and UW data sets are 0.86 and 0.97, compared to −0.18 for ERA-40 and −1.73 for NCEP. This indicates that, on average, 42–97% and 42–86% of the observed discharge trend can be accounted by trends in precipitation from the UW and UDel data sets, respectively, and hence that precipitation trend probably plays a significant role in driving discharge trend in Northern Eurasia.

3.2. Role of Precipitation in Discharge Increases, 1936–1999 (66 Basins)

[28] If precipitation is a driver of observed discharge changes between 1936 and 1999, then substantial agreement between precipitation and discharge trends over that period should exist. This anticipated relationship is borne out in Figure 9, which shows a positive relationship between UDel precipitation and discharge trends with a coefficient of determination (R^2) of 0.43. The coefficient of determination increases to 0.44 when only those basins for which discharge experienced a statistically significant trend are considered. Figure 10a shows basins with statistically significant trends in discharge (40 basins), while Figure 10b shows basins with significant precipitation trends (also 40 basins). The two largely agree, with 24 basins in agreement and 5 in opposition. There are also 11 basins with statistically significant trends in runoff but no statistically significant trends in precipitation, which are also included in the remainder of our analysis. Table 3 shows discharge and precipitation trends for all 66 basins considered. Maximum and minimum discharge trends are −41% and 50%, respectively, and the mean increase is 6%, nearly identical to the 7% increase identified by *Peterson et al.* [2002] for the Eurasian Arctic as a whole. When only basins with statistically significant trends are included, the mean increases to 11%.

[29] As in section 2.4, we calculate R_p for each basin to determine the proportion of discharge trend that could be driven by the observed trend in precipitation (Table 4). The median R_p for those basins with significant trends in discharge (40 of 66 basins) is 0.35, while the median value of $\Delta P/\Delta R$ is 0.62, suggesting that a substantial portion of discharge trend may be related to precipitation changes. For positively correlated basins, R_p ranges from 0.04 to 2.15 with a median value of 0.44. From the spatial distribution of R_p, precipitation and discharge trend appear to be particularly closely associated in European Russia and portions of Eastern Siberia (Figure 11). Basins in which precipitation and discharge trends diverge (8 basins) are scattered throughout the study area with no discernable spatial

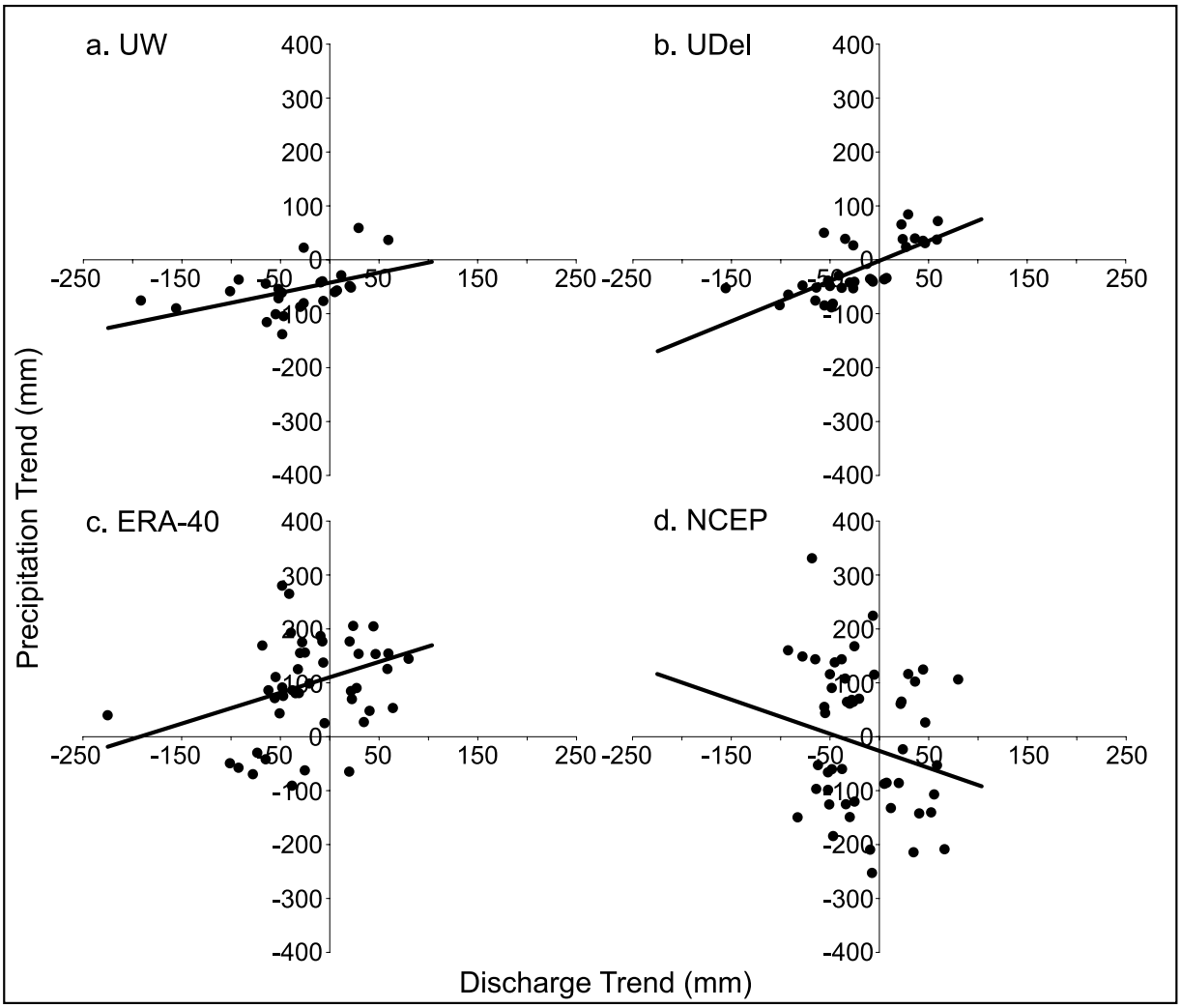

Figure 7. Statistically significant ($p = 0.80$) discharge and precipitation trends for the (a) UW, (b) UDel, (c) ERA-40, and (d) NCEP data sets between 1958 and 1989. River discharge trends are correlated with UW and especially UDel precipitation trends ($R^2 = 0.22$ and 0.49, respectively), while ERA-40 and NCEP show little relation to discharge ($R^2 = 0.09$ and 0.02).

pattern. Finally, in Figure 12 we plot annual discharge trend against watershed ground ice content. No statistically significant linear trend exists in the data ($r^2 = 0.03$), suggesting that permafrost is probably not the main driver of discharge trend over this period. It is notable, however, that the 7 basins with the highest ground ice content show statistically significant increases in discharge. These basins, the Yana, Olenek, Bokhalcha, Amga, Tobol, Adycha, Izhma, and Rybnitsa, and others like them may support an influence of permafrost on river discharge trend in regions with high ground ice content [*Adam et al.*, 2005]. Nonetheless, we find no statistically significant difference in discharge trend between those basins with less than 1% ground ice and those with 4% or more.

4. Discussion and Conclusions

4.1. Precipitation Data Set Comparison

[30] Our fine-scale analysis of 198 basins reveals substantial differences among the UDel, UW, ERA-40, and NCEP precipitation data sets, both when they are compared with each other and also with basin discharge. Overall, ERA-40 displays the weakest relationship between mean annual basin precipitation and mean annual basin runoff (Figure 2c). By contrast, the other three data sets all have similar regression slopes, though their coefficients of determination are generally low, especially NCEP. In terms of magnitude, NCEP is also highest of the four data sets, averaging more than 70% higher than UDel for the 198 basins (Table 2).

[31] The UW and UDel data sets are highly correlated, an unsurprising result since the UW data set is derived from the UDel data. However, significant portions of the ERA-40 and NCEP data sets show little correlation with the two interpolated data sets or with each other (Figure 3). The two reanalysis data sets also have significantly lower levels of correlation with discharge, well below that predicted by *Milly and Dunne* [2002] for all but the driest basins. In particular, ERA-40 displays little correlation with discharge in much of central and northeastern Siberia, while NCEP

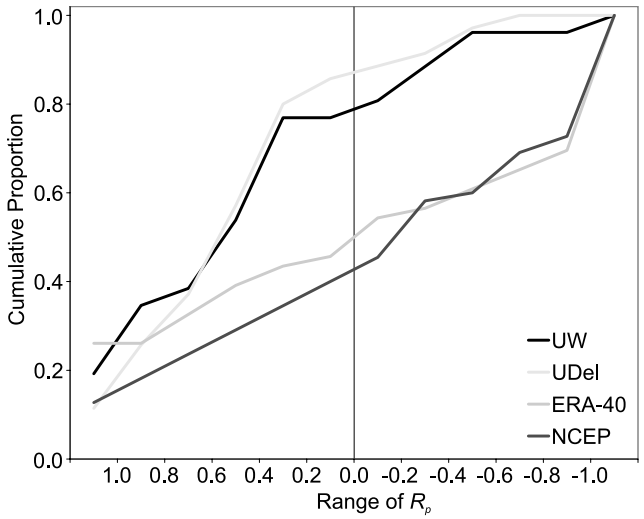

Figure 8. Distributions of the metric R_p, measuring the proportion of observed discharge trend associated with precipitation trend for the UDel, UW, ERA-40, and NCEP data sets over the period 1958 to 1989. The UW and UDel distributions contain relatively few basins with negative values of R_p, while the ERA-40 and NCEP data sets are marked by large negative values of R_p in many basins.

shows only minimal correlation with discharge in much of the Ob' Basin. In addition, spatial patterns in NCEP and ERA-40 precipitation trend often oppose patterns of discharge trend, whereas UW and UDel trends match discharge trends more closely. This effect is also reflected in the median values of R_p and $\Delta P/\Delta R$ for all four precipitation data sets, with the UW and UDel trends showing closer agreement with discharge trends than does either reanalysis product. Taken together, these two findings lead us to conclude that the UW and UDel interpolated data sets substantially outperform the ERA-40 and NCEP data sets, at least in terms of fine-scale spatial phenomena important to watershed hydrology studies. Both of the reanalysis products appear questionable in some areas (the Ob' Basin for NCEP and central and eastern Siberia for ERA-40), though often not in the same areas. The dramatic increases in ERA-40 precipitation over the period of observation (Figure 5c) are probably unrealistic in that they are not corroborated by the discharge records. It is possible that these increases result from the addition of satellite-derived observations to the ERA-40 reanalysis beginning in 1979 [*Adam et al.*, 2005], and recent studies suggest that ERA-40 may perform substantially better after 1979 [*Serreze et al.*, 2005]. The negative relationship and low coefficient of determination between NCEP precipitation and discharge is similarly troubling.

[32] Overall, our results suggest that the use of precipitation time series derived from current reanalysis projects is less preferable than observational data at the fine spatial scales and in the basins examined here between 1958 and 1989. However, the addition of satellite-derived measurements to both the ERA-40 and NCEP reanalysis products beginning in 1979, coupled with the decrease in observation records in the Eurasian Arctic beginning approximately a decade later suggests that reanalysis products may hold increasing value for studies beginning after 1979. In particular, the ERA-40 precipitation product has been shown to have substantial promise in the Eurasian Arctic at larger spatial scales [*Serreze et al.*, 2005]. As such, we recommend that ERA-40 precipitation data be considered alongside observational data for any study encompassing the modern satellite era. Finally, an important implication of this paper is that river discharge may be useful as an independent validation data set for continued improvement of climate reanalysis products. Such products are critical given shrinking numbers of high-latitude ground stations in Russia [*Shiklomanov et al.*, 2002].

[33] The contrast between the UDel and UW interpolated data sets is much more subtle. As anticipated, they are highly correlated and show similar spatial patterns of correlation, both with other precipitation data sets and with river discharge. However, the multiplicative and additive offsets applied to the UW product lead to, on average, 33% higher mean precipitation as compared to UDel data. These offsets do result in differences in trend as well as runoff ratio between the two data sets, leading to somewhat different values of R_p and $\Delta P/\Delta R$ for individual basins. However, the distribution and median values of R_p and $\Delta P/\Delta R$ are quite similar for the two data sets. The improvements in the UW data set over UDel are most evident in Figure 2. Assuming values of between 180 and 400 mm/yr for evapotranspiration in northern Eurasia [*Serreze et al.*, 2003], UDel precipitation values are insufficient to close the water balance in many cases, whereas UW values more closely match expected precipitation values estimated from runoff and evapotranspiration components of the water balance. Therefore the incorporation of the UW data set could help resolve the P-ET deficit observed by *Serreze et al.* [2003] in many areas of northern Eurasia.

4.2. Discharge and Precipitation Variability

[34] A physical explanation for the increases in Eurasian river discharge to the Arctic Ocean observed by *Peterson et al.* [2002] and others has remained elusive to date. *McClelland et al.* [2004] show that permafrost melt, increased fire frequency, and dam construction cannot reasonably play more than minor roles in driving observed discharge changes, whereas *Zhang et al.* [1999, 2000] and *Oelke et al.* [2004] suggest that permafrost may yet be important. Other anthropogenic impacts such as widespread agriculture in portions of the Ob' and Yenisey basins may also influence long-term discharge trends [*Berezovskaya et al.*, 2004; *Yang et al.*, 2004a]. In addition, long-term changes in evapotranspiration (ET) may have affected the water balance in some areas of the Eurasian Arctic [*Ye et al.*, 2004; *Berezovskaya et al.*, 2004], though ET is very difficult to model or measure correctly and any trends are poorly resolved in existing data sets [*Serreze et al.*, 2000, 2003].

[35] Precipitation increase remains a logical candidate mechanism, though past studies have been unable to show substantial relationships between precipitation and discharge trend over the largest river basins in northern Eurasia [e.g., *Berezovskaya et al.*, 2004; *Ye et al.*, 2004]. *Dery and Wood* [2005], however, have shown such a link between discharge and precipitation trends in Arctic Canada. Our approach differs from these earlier efforts by using a statistical approach for long-term records (1936–1999) over

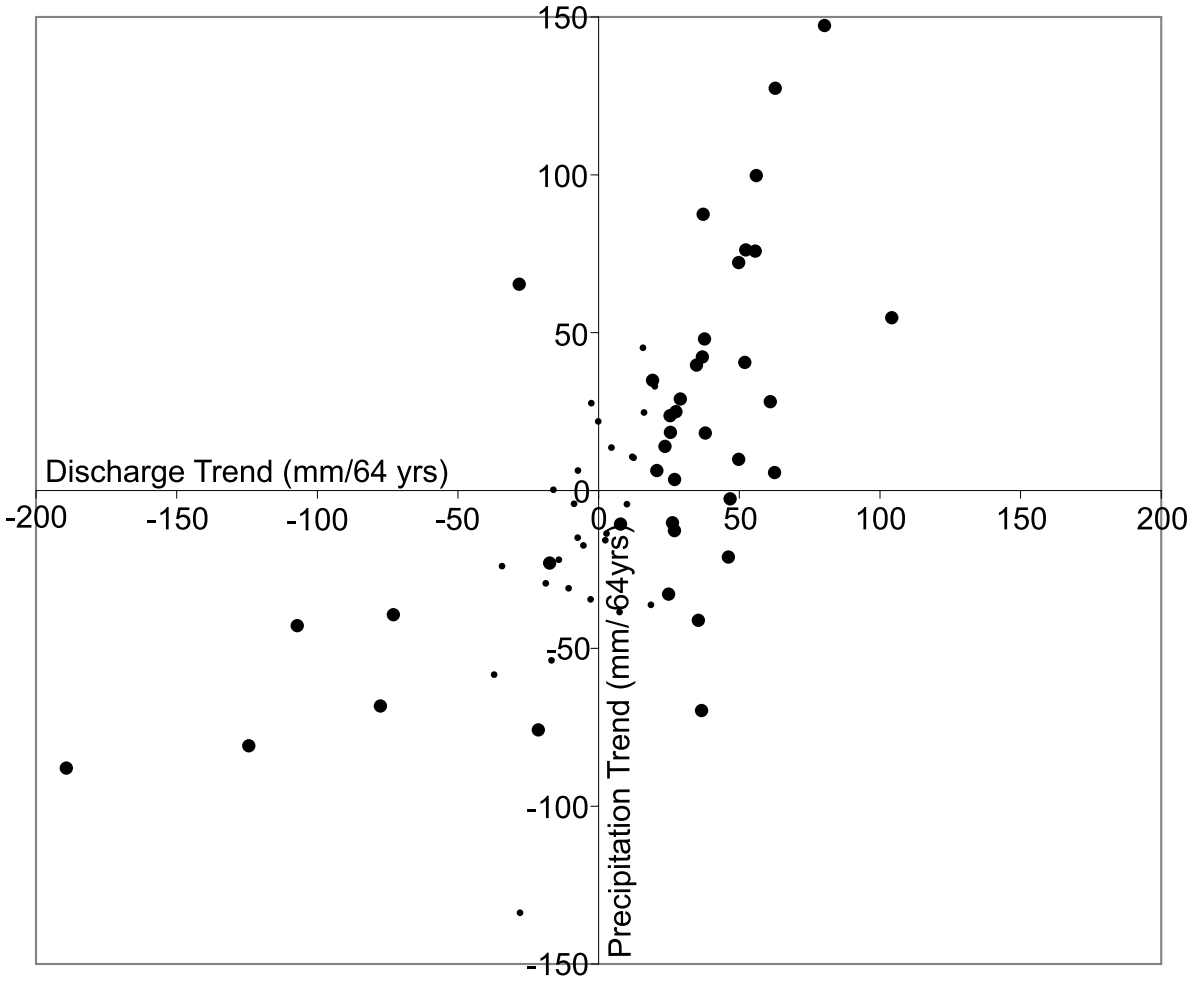

Figure 9. Discharge and UDel precipitation trends over the period 1936–1999 from least squares regression analysis. Those basins in which discharge is statistically significant at the $p = 0.80$ level are in bold. The coefficient of determination (R^2) is 0.44 when only the statistically significant basins are considered.

66 basins. The precipitation data set intercomparison in the first part of this paper indicates that the observationally based UDel and UW data sets are most appropriate for watershed-scale studies of river discharge. Fortunately, the UDel is the longest running of the four, lending confidence to its use for long-term analysis of 66 basins for which discharge records are available.

[36] Substantial agreement is found between discharge and UDel precipitation trends for these 66 basins (Figure 9). Nearly half ($R^2 = 0.44$) of the variability in discharge trend is associated with variability in UDel precipitation trend. In addition, nearly 60% (23 of 40) of river basins with statistically significant trends in river discharge also have statistically significant trends in UDel precipitation in the same direction. The spatial patterns of discharge and precipitation trend also agree in many areas, particularly in European Russia and in some portions of Southern Siberia (Figures 10a–10b). Best agreement is often found in populous areas where more precipitation measurements are presumably collected. This leads us to speculate that similar agreement could possibly be found in more remote northern areas if better precipitation gauging capacity existed. The median values of R_p (0.35) and $\Delta P/\Delta R$ (0.62) for basins with statistically significant discharge trends suggest that between one and two thirds of the observed discharge trend can be explained by changes in precipitation, at least in the basins studied here. It should be noted that more than 55% of the Eurasian Arctic drainage lies outside our study basins and thus may behave differently than those regions examined here. At the same time, we believe that our study area is sufficiently large and diverse to allow speculation on trends in the Eurasian Arctic drainage, though not the Arctic drainage as a whole. A more precise understanding of how ET rates change as precipitation increases or decreases would substantially aid in our examination of the discharge-precipitation relationship. Absent a more complete understanding of ET processes, we offer a range of possible values for the contribution of precipitation to observed discharge trends that depend upon whether ET changes or remains constant with changing precipitation. We anticipate that future research in this area would further refine the precision of our analysis.

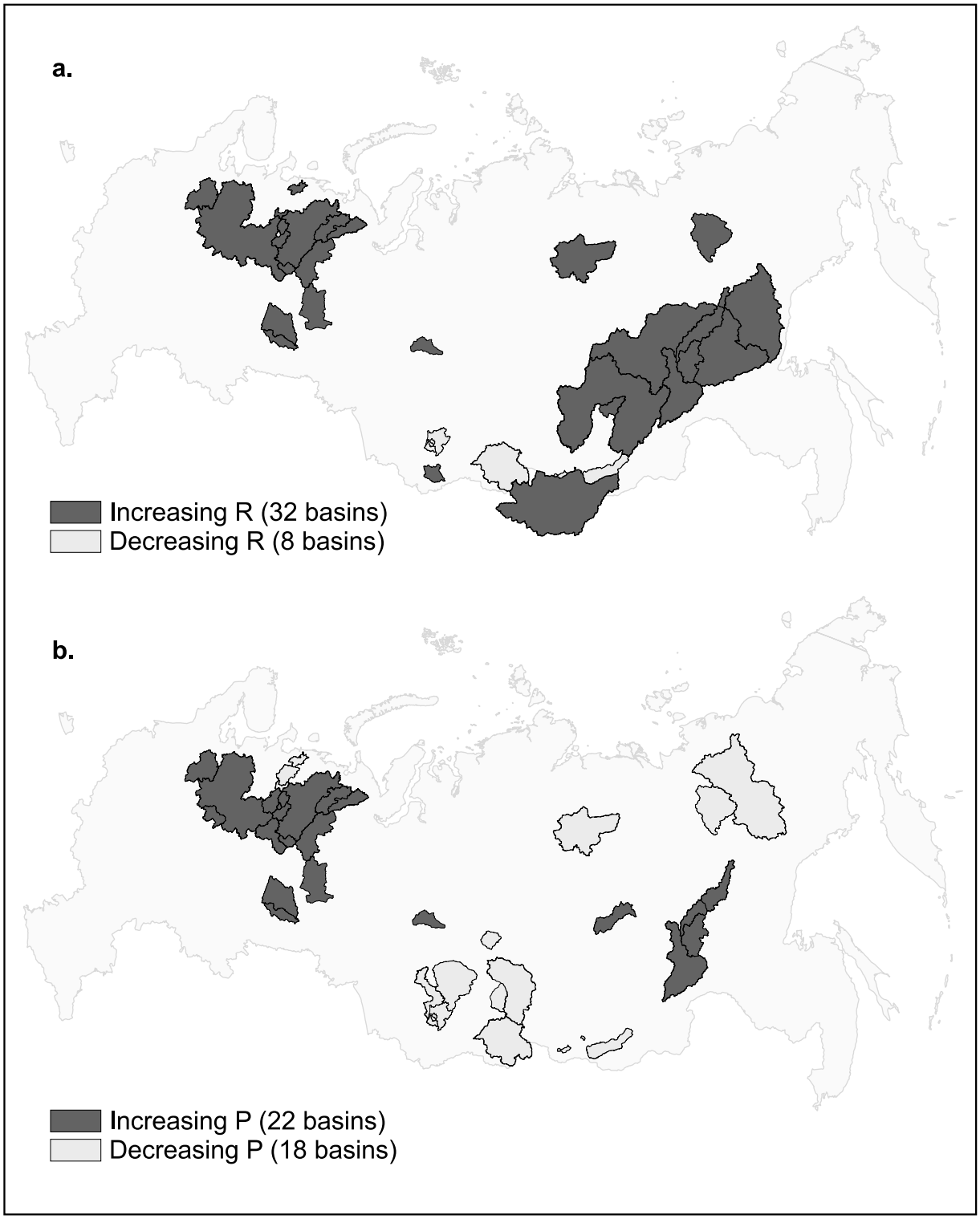

Figure 10. Statistically significant increasing (dark) and decreasing (light) trends in (a) UDel precipitation and (b) river discharge over the period 1936 to 1999. Note the spatial agreement between the two maps, particularly in European Russia and areas of Southern Siberia.

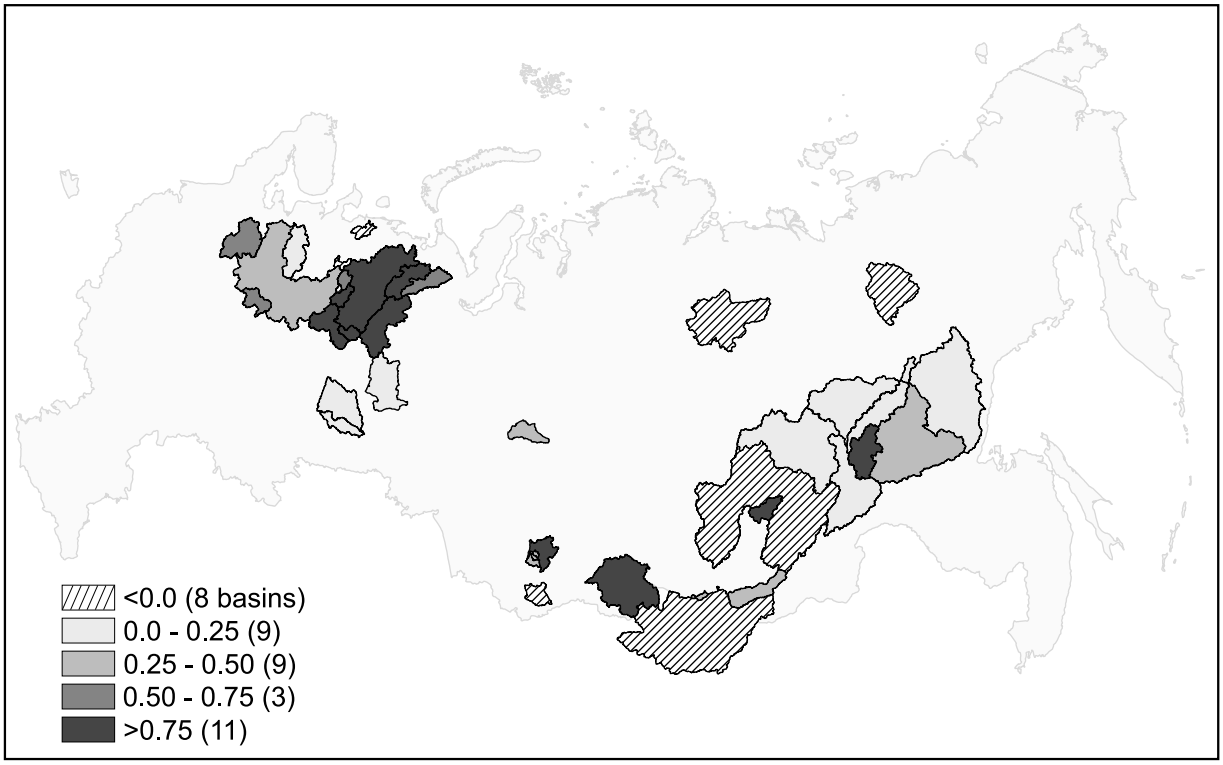

Figure 11. R_p values are mapped for those basins in which discharge trends are statistically significant at the $p = 0.80$ level. Positive values of R_p cluster in European Russia and portions of Easter Siberia, while negative values of R_p, indicating opposing trends, are evenly distributed throughout the study area.

[37] Some recent analyses have questioned the link between precipitation and discharge, suggesting instead that a variety of factors including permafrost thaw may play substantial roles in driving observed discharge changes [*Adam et al.*, 2005; *Zhang et al.*, 1999, 2000; *Oelke et al.*, 2004]. However, the methods used by *Adam et al.* [2005], including macroscale hydrologic modeling, a focus on large basins, and an examination of discharge-precipitation relationships over a large number of different time steps, are sufficiently different from those used in our analysis that the two studies may both be valid. Future studies should resolve these differing conclusions. Given the uncertain quality of available precipitation data, we believe that broad-scale, statistical analyses for large numbers of basins will lead to the most conclusive results.

[38] Our own study of 66 unregulated basins suggests a substantial role for precipitation in driving observed changes in river runoff. The same cannot be said for permafrost, where no clear relationship between runoff and basin permafrost extent is observed. Also, the large number of river basins containing little or no ground ice but showing statistically significant discharge increases suggests that some other mechanism must be at work. Still, the presence of ground ice may affect discharge trends in certain limited areas as suggested by the pervasive increases observed in basins with the highest ground ice content. Additionally, changes in permafrost extent and active layer thickness undoubtedly influence many aspects of the Arctic hydrologic cycle on seasonal timescales [*Oelke et al.*, 2004], so permafrost thaw and other mechanisms may contribute to discharge variability. It seems likely, however, that increased annual precipitation has played an eminent role in the observed 20th century increases in Eurasian river runoff.

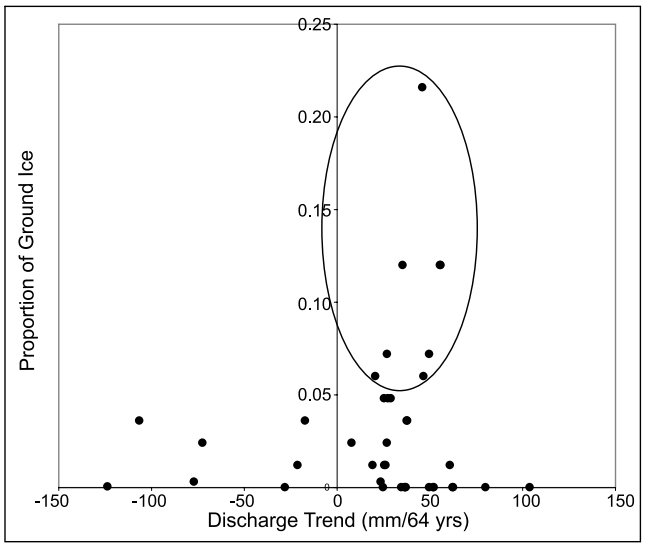

Figure 12. Proportion of ground ice plotted against statistically significant ($p = 0.80$) trends in river discharge for 1936–1999 (n = 40). No statistically significant pattern is evident ($r^2 = 0.02$), though the 7 basins (circled) with the highest ground ice content show statistically significant increases in discharge, suggesting some influence.

[39] **Acknowledgments.** Funding for this research was provided by the NSF Arctic System Science Program (ARCSS) Freshwater Initiative (ARC-023091). We thank D. Lettenmaier, J. Adam, C. Lammers, and A. Shiklomanov for access to precipitation and river discharge data and K. Sampson for his input in early stages of the research. Finally, we thank M. Serreze and A. Barrett for their input and assistance.

References

Aagard, K., and E. C. Carmack (1989), The role of sea ice and other fresh water in the Arctic circulation, *J. Geophys. Res.*, *94*, 14,485–14,498.

Adam, J. C., and D. P. Lettenmaier (2003), Adjustment of global gridded precipitation for systematic bias, *J. Geophys. Res.*, *108*(D9), 4257, doi:10.1029/2002JD002499.

Adam, J. C., F. Su, and D. P. Lettenmaier (2005), Exploring the effects of precipitation changes on the variability of pan-Arctic river discharge, *Eos Trans. AGU*, *86*(52), Fall Meet. Suppl., Abstract U41A-0812.

Adam, J. C., E. A. Clark, D. P. Lettenmaier, and E. F. Wood (2006), Correction of global precipitation products for orographic effects, *J. Clim.*, *19*(1), 15–38.

Arctic Climate Impact Assessment (ACIA) (2005), *Arctic Climate Impact Assessment*, Cambridge Univ. Press, New York.

Berezovskaya, S., D. Yang, and D. L. Kane (2004), Compatibility analysis of precipitation and runoff trends over the large Siberian watersheds, *Geophys. Res. Lett.*, *31*, L21502, doi:10.1029/2004GL021277.

Brown, J., et al. (1998), *Circum-Arctic Map of Permafrost and Ground-Ice Conditions*, World Data Cent. for Glaciol., Natl. Snow and Ice Data Cent., Boulder, CO. (http://nsidc.org/data/ggd318.html).

Bryden, H. L., H. R. Longworth, and S. A. Cunningham (2005), Slowing of the Atlantic meridional overturning circulation at 25 degrees N, *Nature*, *438*(7068), 655–657, doi:10.1038/nature04385.

Burn, D. H. (1994), Hydrologic effects of climatic change in west-central Canada, *J. Hydrol.*, *160*, 53–70.

Curry, R., B. Dickson, and I. Yashayaev (2003), A change in the freshwater balance of the Atlantic Ocean over the past four decades, *Nature*, *426*, 826–829, doi:10.1038/nature02206.

Dery, S., and E. Wood (2004), Teleconnection between the Arctic Oscillation and Hudson Bay river discharge, *Geophys. Res. Lett.*, *31*, L18205, doi:10.1029/2004GL020729.

Dery, S., and E. Wood (2005), Decreasing river discharge in northern Canada, *Geophys. Res. Lett.*, *32*, L10401, doi:10.1029/2005GL022845.

Dickson, B., I. Yashayaev, J. Meincke, B. Turrel, S. Dye, and J. Holfort (2002), Rapid freshening of the deep North Atlantic Ocean over the past four decades, *Nature*, *416*, 832–837, doi:10.1038/416832a.

Fekete, B. M., C. J. Vorosmarty, J. O. Roads, and C. J. Willmott (2004), Uncertainties in precipitation and their impacts on runoff estimates, *J. Clim.*, *17*, 294–304.

Gedney, N., P. M. Cox, R. A. Betts, O. Boucher, C. Huntingford, and P. A. Scott (2006), Detection of a direct carbon dioxide effect in continental river runoff records, *Nature*, *439*, 838–841, doi:10.1038/nature04504.

Georgievskii, V. Y., A. V. Ezhov, A. L. Shalygin, I. A. Shiklomanov, and A. I. Shiklomanov (1996), Assessment of the effect of possible climate changes on hydrological regime and water resources of rivers in the former USSR, *Russ. Meteorol. Hydrol.*, *11*, 66–74.

Groisman, P. Y., and E. Y. Rankova (2001), Precipitation trends over the Russian permafrost-free zone: Removing the artifacts of pre-processing, *Int. J. Climatol.*, *21*, 657–678.

Groisman, P. Y., V. V. Koknaeva, T. A. Belokrylova, and T. R. Karl (1991), Overcoming biases of precipitation measurement: A history of the USSR experience, *Bull. Am. Meteorol. Soc.*, *72*, 1725–1733.

Hamlet, A. F., and D. P. Lettenmaier (2005), Production of temporally consistent gridded precipitation and temperature fields for the continental United States, *J. Hydrometeorol.*, *6*, 330–336, doi:10.1175/JHM420.1.

Hinzman, L. D., et al. (2005), Evidence and implications of recent climate change in northern Alaska and other Arctic regions, *Clim. Change*, *72*, 251–298, doi:10.1007/s10584-005-5352-2.

Hirsch, R. M., R. B. Alexander, and R. A. Smith (1991), Selection of methods for the detection and estimation of trends in water quality, *Water Resour. Res.*, *27*, 803–813.

Hodgkins, G. A., R. W. Dudley, and T. G. Huntington (2005), Changes in the number and timing of days of ice-affected flows on northern New England rivers, 1930–2000, *Clim. Change*, *71*, 319–340, doi:10.1007/s10584-005-5926-z.

Intergovernmental Panel on Climate Change (IPCC) (2001), *Climate Change 2001: The Scientific Basis; Contribution of Working Group I to the Third Assessment Report of the IPCC*, edited by J. C. Houghton et al., 881 pp., Cambridge Univ. Press, New York.

Kattsov, V. M., and J. E. Walsh (2000), Twentieth-century trends of Arctic precipitation from observational data and a climate model simulation, *J. Clim.*, *13*, 1362–1370.

Kendall, M. G. (1975), *Rank Correlation Methods*, 4th ed., Oxford Univ. Press, New York.

Kistler, R., et al. (2001), The NCEP-NCAR 50 year reanalysis: Monthly means CD-ROM and documentation, *Bull. Am. Meteorol. Soc.*, *82*, 247–267.

Lammers, R. B., A. I. Shiklomanov, C. J. Vorosmarty, B. M. Fekete, and B. J. Peterson (2001), Assessment of contemporary Arctic river runoff based on observational discharge records, *J. Geophys. Res.*, *106*, 3321–3334.

Lawrence, D. M., and A. G. Slater (2005), A projection of severe near-surface permafrost degradation during the 21st century, *Geophys. Res. Lett.*, *32*, L24401, doi:10.1029/2005GL025080.

Legates, D. R., and G. J. McCabe (1999), Evaluation the use of "goodness-of-fit" measures in hydrologic and hydroclimatic model validation, *Water Resour. Res.*, *35*, 233–241.

Lins, H. F., and J. R. Slack (1999), Streamflow trends in the United States, *Geophys. Res. Lett.*, *26*, 227–230.

Maidment, D. R. (Ed.) (1993), *Handbook of Hydrology*, McGraw-Hill, New York.

Manabe, S., and R. J. Stouffer (1995), Simulation of abrupt climate-change induced by fresh-water input to the North Atlantic Ocean, *Nature*, *278*(6553), 165–167.

Manabe, S., P. C. D. Milly, and R. Wetherald (2004), Simulated long-term changes in river discharge and soil moisture due to global warming, *Hydrol. Sci. J.*, *49*, 625–642.

Mann, H. B. (1945), Non-parametric test against trend, *Econometrica*, *13*, 245–259.

McClelland, J. W., R. M. Holmes, B. J. Peterson, and M. Stieglitz (2004), Increasing river discharge in the Eurasian Arctic: Consideration of dams, permafrost thaw, and fires as potential agents of change, *J. Geophys. Res.*, *109*, D18102, doi:10.1029/2004JD004583.

Milly, P. C. D., and K. A. Dunne (2002), Macroscale water fluxes: 2. Water and energy supply control of their interannual variability, *Water Resour. Res.*, *38*(10), 1206, doi:10.1029/2001WR000760.

Oelke, C., T. J. Zhang, and M. C. Serreze (2004), Modeling evidence for recent warming of the Arctic soil thermal regime, *Geophys. Res. Lett.*, *31*(7), L07208, doi:10.1029/2003GL019300.

Peterson, B. J., R. M. Holmes, J. W. McClelland, C. J. Vorosmarty, R. B. Lammers, A. I. Shiklomanov, and S. Rahmstorf (2002), Increasing river discharge to the Arctic Ocean, *Science*, *298*, 2171–2173.

Rahmstorf, S. (1995), Bifurcations of the Atlantic thermohaline circulation in response to changes in the hydrologic cycle, *Nature*, *378*(6553), 145–149.

Rawlins, M. A., R. B. Lammers, S. Frolking, B. M. Fekete, and C. J. Vorosmarty (2003), Simulating pan-Arctic runoff with a macro-scale terrestrial water balance model, *Hydrol. Processes*, *17*, 2521–2539, doi:10.1002/hyp.1271.

Rawlins, M. A., C. J. Willmott, A. Shiklomanov, E. Linder, S. Frolking, and R. B. Lammers (2006), Evaluation of trends in derived snowfall and rainfall across Eurasia and linkages with discharge to the Arctic Ocean, *Geophys. Res. Lett.*, *33*(7), L07403, doi:10.1029/2005GL025231.

Serreze, M. C., and A. J. Etringer (2003), Precipitation characteristics of the Eurasian Arctic drainage system, *Int. J Climatol.*, *23*(11), 1267–1291.

Serreze, M. C., J. E. Walsh, F. S. Chapin, T. Osterkamp, M. Dyurgerov, V. Romanovsky, W. C. Oechel, J. Morison, T. Zhang, and R. T. Barry (2000), Observational evidence of recent change in the northern high-latitude environment, *Clim. Change*, *46*, 159–207.

Serreze, M. C., D. H. Bromwich, M. P. Clark, A. J. Etringer, T. Zhang, and R. B. Lammers (2002), Large-scale hydro-climatology of the terrestrial Arctic drainage system, *J. Geophys. Res.*, *108*(D2), 8160, doi:10.1029/2001JD000919.

Serreze, M. C., M. P. Clark, and D. H. Bromwich (2003), Monitoring precipitation over the Arctic terrestrial drainage system: Data requirements, shortcomings, and applications to atmospheric reanalysis, *J. Hydrometeorol.*, *4*, 387–407.

Serreze, M. C., A. Barrett, and F. Lo (2005), Northern high latitude precipitation as depicted by atmospheric reanalyses and satellite retrievals, *Mon. Weather Rev.*, *113*, 3407–3430.

Shiklomanov, A. I., R. B. Lammers, and C. J. Vorosmarty (2002), Widespread decline in hydrologic monitoring threatens pan-Arctic research, *EOS Trans. AGU*, *83*, 13.

Simmons, A. J., and J. K. Gibson (2000), *The ERA-40 Project Plan*, *ECMWF ERA-40 Proj. Rep. Ser. 1*, 63 pp.

Smith, L. C. (2000), Trends in Russian Arctic river-ice formation and breakup, 1917–1994, *Phys. Geogr.*, *20*(1), 46–56.

Steele, M., D. Thomas, and D. Rothrock (1996), A simple model study of the Arctic Ocean freshwater balance, 1979–1985, *J. Geophys. Res.*, *101*, 20,833–20,848.

Willmott, C. J., and K. Matsuura (2001), *Terrestrial Air Temperature and Precipitation: Monthly and Annual Time Series (1950–2001) (version 1. 02)*, Cent. for Clim. Res., Univ. of Del., Newark, N. J.

Wu, P., R. Wood, and P. Stott (2005), Human influence on increasing Arctic river discharges, *Geophys. Res. Lett.*, *32*, L02703, doi:10.1029/2004GL021570.

Yang, D., and T. Ohata (2001), A bias-corrected Siberian regional precipitation climatology, *J. Hydrometeorol.*, *2*, 122–139.

Yang, D., D. L. Kane, L. D. Hinzman, X. Zhang, T. Zhang, and H. Ye (2002), Siberian Lena River hydrologic regime and recent change, *J. Geophys. Res.*, *107*(D23), 4694, doi:10.1029/2002JD002542.

Yang, D. Q., B. Ye, and A. I. Shiklomanov (2004a), Discharge characteristics and changes over the Ob' River watershed in Siberia, *J. Hydrometeorol.*, *5*, 595–610.

Yang, D. Q., B. Ye, and D. L. Kane (2004b), Streamflow changes over Siberian Yenisei River Basin, *J. Hydrol.*, *296*, 59–80, doi:10.1016/j.jhydrol.2004.03.17.

Yang, D. Q., D. Kane, Z. P. Zhang, D. Legates, and B. Goodison (2005), Bias corrections of long-term (1973–2004) daily precipitation data over the northern regions, *Geophys. Res. Lett.*, *32*(19), L19501, doi:10.1029/2005GL024057.

Ye, B., D. Q. Yang, and D. L. Kane (2003), Changes in Lena River streamflow hydrology: Human impacts versus natural variations, *Water Resour. Res.*, *39*(7), 1200, doi:10.1029/2003WR001991.

Ye, H., D. Yang, X. Zhang, and T. Zhang (2003), Connections of Yenisei River discharge to sea surface temperatures, sea ice, and atmospheric circulation, *J. Geophys. Res.*, *108*(D24), 4776, doi:10.1029/2003JD003759.

Ye, H., D. Yang, T. Zhang, X. Zhang, S. Ladochy, and M. Ellison (2004), The impact of climatic conditions on seasonal river discharges in Siberia, *J. Hydrometeorol.*, *5*, 286–295.

Yin, X., A. Gruber, and P. Arkin (2004), Comparison of the GPCP and CMAP merged gauge-satellite monthly precipitation products for the period 1979–2001, *J. Hydrometeorol.*, *5*, 1207–1222.

Zhang, T., R. G. Barry, K. Knowles, J. A. Heginbottom, and J. Brown (1999), Statistics and characteristics of permafrost and ground-ice contribution in the Northern Hemisphere, *Polar Geogr.*, *23*(2), 132–154.

Zhang, T., J. A. Heginbottom, R. G. Barry, and J. Brown (2000), Further statistics on the distribution of permafrost and ground ice in the northern hemisphere, *Polar Geogr.*, *24*(2), 126–131.

T. M. Pavelsky and L. C. Smith, Department of Geography, University of California, Los Angeles, Los Angeles, CA 90095, USA. (pavelsky@ucla.edu)